J|A|C|S
ARTICLES
Published on Web 12/23/2003

Selective Formation of Stable Triplexes Including a TA or a CG Interrupting Site with New Bicyclic Nucleoside Analogues (WNA)

Shigeki Sasaki,*,† Yosuke Taniguchi, Ryo Takahashi, Yusuke Senko, Keiichi Kodama, Fumi Nagatsugi, and Minoru Maeda

Contribution from the Graduate School of Pharmaceutical Sciences, Kyushu University, 3-1-1 Maidashi, Higashi-ku, Fukuoka 812-8582, Japan, and CREST, Japan Science and Technology Agency

Received July 11, 2003; E-mail: sasaki@phar.kyushu-u.ac.jp

Abstract: Triplex-forming oligonucleotides (TFOs) are potential DNA-targeting molecules and would become powerful tools for genomic research. As the stabilization of the TFO is partially provided by hydrogen bonds to purine bases, the most stable triplexes form with homopurine/homopyrimidine sequences, and a pyrimidine base in the purine strand of the duplex interrupts triplex formation. If a TFO can recognize sequences including such an interrupting site, the target regions in the genome would be expanded to a greater extent. However, this problem has not been generally solved despite extensive studies. We have previously reported a new base analogue (WNA) constructed of three parts, a benzene ring, a heterocyclic ring, and a bicyclic skeleton to hold these two parts. In this study, we have further investigated modification of WNA systematically and determined two useful WNA analogues, WNA-βT and WNA-βC, for selective stabilization of triplexes at a TA and a CG interrupting site, respectively. The triplexes with WNA analogues have exhibited an interesting property in that they are more stable than natural-type triplexes even at low Mg^{2+} concentration. From comparison of the results with H-WNA-βT lacking benzene and those with WNA-H without thymine, it has been suggested that benzene is a major contributor for triplex stability and thymine provides selectivity. Thus, it has been successfully demonstrated that WNA-βT/TA and WNA-βC/CG combinations may expand triplex recognition codes in addition to the natural A/AT and G/GC base triplet codes. The results of this study will provide useful information for the design of new WNA analogues to overcome inherent problems for further expansion of triplex recognition codes.

Introduction

DNA-recognizing molecules would become powerful tools for genomic research through gene inhibition, activation, gene conversion and/or recombination, and gene therapy, etc. One potential candidate of great interest has been triplex-forming oligonucleotides (TFOs) and related molecules.[1−7] Recent successful illustrations of the application include the achievement of specific mutations by TFOs in mice, inhibition of cell growth by PEG-TFO conjugates, and so on. There is, however, an intrinsic limitation in the sequences that can be targeted by TFOs.[1,8] As a TFO recognizes DNA sequence by binding the major groove with hydrogen bonds between the bases in the third strand and those in the purine strand of the duplex, the most stable triplexes form on homopurine/homopyrimidine sequences. Even a single pyrimidine base in the purine strand of the duplex interrupts triplex formation to a great extent. If TFOs can recognize sequences including such an interrupting site, their target regions within the genome would be expanded to a greater extent. Despite numerous studies for more than a decade, this limitation has remained an unsolved problem.[9−13]

In triplexes, pyrimidine-TFOs adopt parallel orientation, and purine-TFOs tend toward an antiparallel orientation to the purine strand of the duplex. Recently, interesting nucleoside analogues have been reported from Leumann's and Imanishi's groups, which stabilize parallel triplexes by forming one hydrogen bond to the cytosine base at a C−G interrupting site.[14−17] The bicyclic

† CREST, Japan Science and Technology Agency.

(1) Soyfer, V. N.; Potaman, V. N. *Triple-Helical Nucleic Acids*, Springer-Verlag: New York, 1996.
(2) Rapozzi, V.; Cogoi, S.; Spessotto, P.; Risso, A.; Bonora, G.; Quadrifoglio, F.; Xodo, L. *Biochemistry* **2002**, *41*, 502−510.
(3) Cogoi, S.; Rapozzi, V.; Quadrifoglio, F.; Xodo, L. *Biochemistry* **2001**, *40*, 1135−1143.
(4) Casey, B. P.; Glazer, P. M. *Prog. Nucleic Acid Res. Mol. Biol*. **2001**, *67*, 163−192.
(5) Vasquez, K. M.; Narayanan, L.; Glazer, P. M. *Science* **2000**, *209*, 530−533.
(6) Kuznetsova, S.; Ait-Si-Ali, S.; Nagibneva, I.; Troalen, F.; Le Villain, J.-P.; Harel-Bellan, A.; Svinarchuk, F. *Nucleic Acids Res.* **1999**, 27, 3995−4000.
(7) Stanojevic, D.; Young, R. A. *Biochemistry* **2002**, *41*, 7209−7216.
(8) Moser, H. E.; Dervan, P. B. *Science* **1987**, *238*, 645−650.
(9) Griffin, L. C.; Kiessling, L. L.; Beal, P. A.; Gillespie, P.; Dervan, P. B. *J. Am. Chem. Soc*. **1992**, *114*, 7979−7982.
(10) Huang, C. Y.; Cushman, C. D.; Miller, P. S. *J. Org. Chem.* **1993**, *58*, 5048−5049.
(11) Sasaki, S.; Nakashima, S.; Nagatsugi, F.; Tanaka, Y.; Hisatome, M.; Maeda, M. *Tetrahedron Lett*. **1995**, *36*, 9521−9524.
(12) Rao, T. S.; Hogan, M. E.; Revankar, G. R. *Nucleotides Nucleosides* **1994**, *13*, 95−107.
(13) Parel, S. P.; Leumann, C. J. *Nucleic Acid Res.* **2001**, *29*, 2260−2267.
(14) Buchini, S.; Leumann, C. J. *Tetrahedron Lett*. **2003**, *44*, 5065−5068.

10.1021/ja037211z CCC: $27.50

sugar structure of Imanishi's nucleoside analogues (BNA or LNA) is thought to bring an additional stabilizing effect. Unfortunately, the validity of their design concept has not been proved in a search for nucleoside analogues for a TA interrupting site.

Compared to studies for parallel triplexes, fewer studies have been made for antiparallel triplexes with interrupting sites. An advantage of antiparallel triplexes is that they are formed under neutral conditions with high stability, whereas a disadvantageous point is that their triplex formation is inhibited by physiological ionic conditions, especially in the presence of K^+. We recently developed a new general structure of nucleoside analogues (WNA) with a bicyclo[3.3.0]octane skeleton bearing an aromatic part for stacking and a nucleobase for Hoogesteen hydrogen bonds.[18−20] Our initial success encouraged us to undertake further systematic investigations, and we have determined two useful analogues for selective stabilization of triplexes at a TA or a CG interrupting site. An interesting property of WNA analogues is that the triplex stability with the WNA analogue is higher than that of natural-type triplexes even at low Mg^{2+} concentration. Here, we describe in detail the design, synthesis, and evaluation of the triplex-forming ability of the TFOs incorporating the new base analogues (WNA).

Results

Design. Parallel and antiparallel triplexes differ remarkably from each other in the geometry of the sugar−phosphate backbone. It is anticipated that the backbone of the purine-TFO in the antiparallel triplexes is located at approximately the central position in the major groove, whereas the backbone of the pyrimidine-TFO is much closer to the purine strand of the duplex (Figure 1, A vs B). Taking such a difference into account, nucleoside analogues with C1′-α-glycosidic bond were investigated, but selective formation of triplexes including interrupting sites has not been clearly shown.[13,21] Triplex stability is provided by synchronization of interactions of hydrogen bonds, stacking interactions, shape complimentarity, electrostatic interactions with metal cations, and so on. It may be speculated that a nucleobase with C1′-α stereochemistry might not adopt the appropriate position for hydrogen bonds to the target base pair (Figure 1C). It seemed to us that an appropriate spacer is needed to bring a nucleobase so as to interact with a distant purine base in the pyrimidine strand. Therefore, we designed new nucleoside analogues with an appropriate spacer. Our basic concept for the design of the new nucleoside analogue is schematically illustrated in Figure 2 using WNA-7βG as an example.

Based on molecular modeling, an ethylene spacer with C1′-α stereochemistry was designed to connect a nucleobase unit for hydrogen bonds to a distant purine base (Figure 2A). Conformation of a nucleobase unit might become restricted by construction of a bicyclic ring (Figure 2B). Finally, we considered that a benzene ring at the C1′-β position might occupy a space where a base unit of a natural nucleoside is located and provide stacking and/or van der Waals interactions (Figure 2C). A simulated structure of the triplex including a WNA-7βG and a TA interrupting site suggested that a benzene ring of WNA-7βG might be stacked between adjacent purine bases of the TFO (Figure 3A). It was also predicted that a benzene ring together with a nucleobase might provide a shape complementary to a TA base pair (Figure 3B). Thus, we proposed an original approach of separating the hydrogen-bonding and base-stacking contributions into triplex formation at the interrupting sites. As a benzene ring, a five-membered ring and a nucleobase seem to be aligned in a W-shape; we named the new molecule W-shape nucleoside analogue (WNA) with the number (as necessary) and α or β to represent the alkylation position of the nucleobase and the stereochemistry of its glycosidic bond, respectively. In the preliminary study, the validity of this molecular design was demonstrated by the fact that the TFO incorporating WNA-7βG (**2b**) forms the triplex toward the duplex with a TA interrupting site.[18]

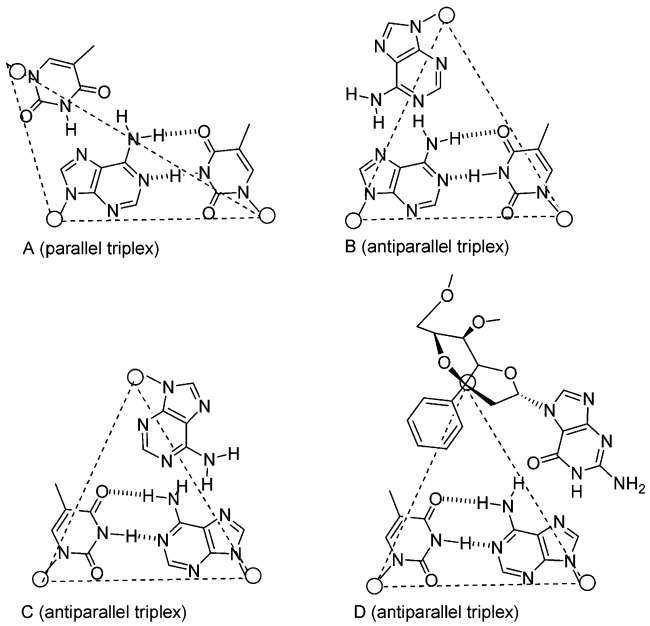

Figure 1. Schematic illustration of difference in backbone geometry of parallel and antiparallel triplex. Circles represent the position of C1′. (A) T-AT triplet, (B) A-AT triplet, (C) an anticipated triplet of C1′ αA-TA, (D) an anticipated triplet of WNA-7βG-TA.

Encouraged by the initial success with WNA-7βG (**2b**),[18] we undertook further systematic investigation with a variety of WNA analogues by altering the nucleobase unit. The compounds used in this study are shown in Figure 4.

Synthesis. The WNA derivatives were synthesized with D-ribose by a modification of the previously reported method[18] (Scheme 1). The intermediate having a benzene ring at the 1-position (**10**) was prepared by a multistep synthesis including protection of the 2,3-dihydroxyl group with acetonide, selective protection of the 5-hydroxyl group with the TBDMS group, oxidation of the 1-hydroxyl group to carbonyl,[22] and addition of phenyllithium. Allylation at the 1-position gave **11** in a ratio

(15) Prevot-Halter, I.; Leumann, C. J. *Bioorg. Med. Chem. Lett.* **1999**, *9*, 2657−2660.
(16) Hari, Y.; Obika, S.; Sekiguchi, M.; Imanishi, T. *Tetrahedron* **2003**, *59*, 5123−5128.
(17) Obika, S.; Hari, Y.; Sekiguchi, M.; Imanishi, T. *Angew. Chem., Int. Ed.* **2001**, *40*, 2079−2081.
(18) Sasaki, S.; Yamauchi, H.; Nagatsugi, F.; Takahashi, R.; Taniguchi, Y.; Maeda, M. *Tetrahedron Lett.* **2001**, *42*, 6915−6918.
(19) Sasaki, S.; Yamauchi, H.; Takahashi, R.; Taniguchi, Y.; Maeda, M. *Nucleic Acids Res. Supp.* **2001**, *1*, 23−24.
(20) Taniguchi, Y.; Takahashi, R.; Kodama, K.; Senko, Y.; Maeda, M.; Sasaki, S. *Nucleic Acids Res. Supp.* **2002**, *2*, 35−36.
(21) Thuong, N. T.; Helene, C. *Angew. Chem., Intl. Ed. Engl.* **1993**, *32*, 666−690.
(22) Ogura, H.; Takahashi, H.; Itoh, T. *J. Org. Chem.* **1972**, *37*, 72−75.

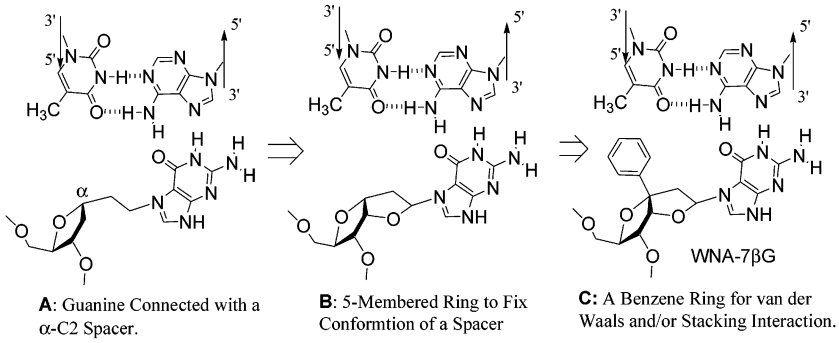

Figure 2. Design of a bicyclic structure having a base and a benzene ring.

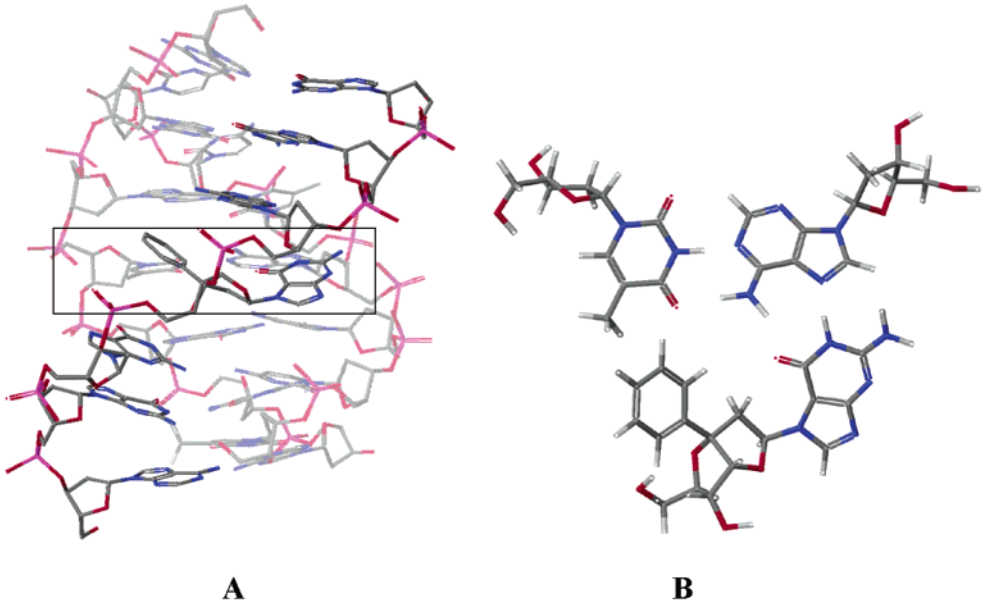

Figure 3. Expected structure of triplex with a WNA-7βG/TA interrupting site. The square indicates the area of WNA-7βG/TA (A), the triplet structure of which is shown in part B.

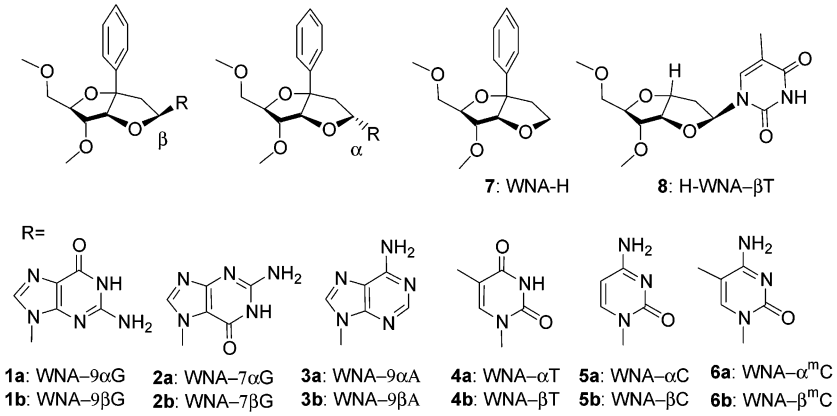

Figure 4. Structures of the WNA (W-shape nucleoside analogue). The number, α, or β represent the position of the nucleobase for glycosidic bond and its stereochemistry, respectively.

of α:β = 7:6 for the stereochemistry of the allyl group, which was used for the following reaction without separation. Subsequently, oxidative cleavage of the vinyl group and subsequent deprotection of 2,3-*O*-acetonide spontaneously provided the corresponding bicyclo[3.3.0]octane derivative, then the formed hydroxyl groups were acetylated to afford the key intermediate **12**. The cyclic compound **12** was easily separated from the noncyclic compound which was derived from **11** with undesired β-allyl stereochemistry. A similar hemiketal intermediate (**14**) lacking a benzene ring was synthesized by a similar sequence of reactions from **13**.[23]

N-Glycosidation to **12** with the corresponding base derivatives was done under different conditions to produce a mixture of 7-*N* and 9-*N* alkylated isomers in the synthesis of **16** and **17**

(23) Mukaiyama, T.; Kobayashi, S. *Carbohydr. Res.* **1987**, *171*, 81−87.

Scheme 1 [a]

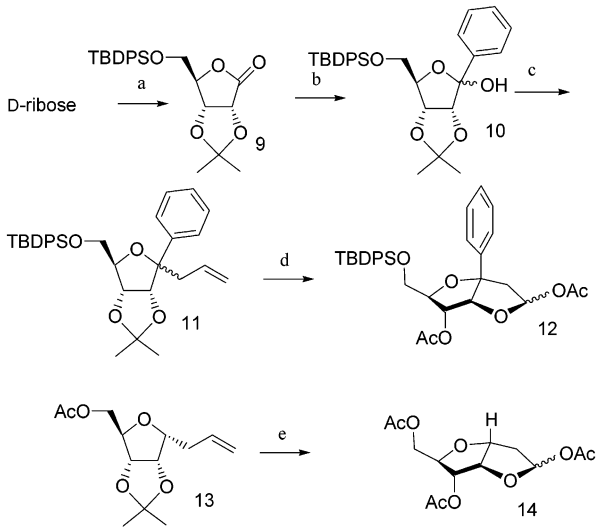

[a] (a) (1) acetone, H^+, (2) TBDPSCl, TEA, DMAP, CH_2Cl_2, (3) PCC, CH_2Cl_2, (b) PhLi, THF, (c) allyltrimethylsilane, $ZnBr_2$, CH_3NO_2, (α:β = 7:6), (d) (1) OsO_4, $NaIO_4$, pyridine, (2) 5% H_2SO_4, THF, (3) Ac_2O, pyridine, (e) (1) OsO_4, $NaIO_4$, pyridine, (2) 2 M HCl−THF, (3) Ac_2O, pyridine.

and α- and β-isomers in all syntheses, which were separated by flash chromatography (Scheme 2).[24,25] Regioisomers of 7-*N* and 9-*N* alkylation were determined based on a comparison of the chemical shift values of the ^{1}H and ^{13}C NMR spectra.[26,27] The stereochemistry of the isolated isomers was determined by ^{1}H-COSY and NOESY spectra.[28] The abasic-type WNA-H was prepared from **12** via reduction with Et_3SiH and TMSOTf. H-WNA-βT was similarly prepared from **14**.

Each isomer of the new nucleoside analogues was transformed to the corresponding amidite precursor with a 5′-*O*-dimethoxytrity (DMTr) protecting group and incorporated into the TFOs by an automated DNA synthesizer. DNA synthesis was carried out by the conventional method using DCI as the activator, TCA for deprotection of the DMTr group, and iodine as the oxidizer. Cleavage of the DMTr-bearing TFOs from the resin and removal of the protecting groups were performed by heating in 28% NH_4-OH, followed by purification by HPLC with an ODS column. Subsequently, deprotection of DMTr was done in 10% acetic acid, and the structure and purity of the obtained TFO were confirmed by MALDI-TOF MASS measurements. The target duplexes were formed by annealing and purified by HPLC.

Evaluation of Triplex Formation. Triplexes were formed by incubating the TFO, the ^{32}P-labeled TFO as a tracer and the duplex for 12 h at 22 °C in a buffer containing 20 mM Tris-HCl, 20 mM $MgCl_2$, 2.5 mM spermidine and 10% sucrose at pH 7.5. The triplex formed was evaluated by gel shift assay with 15% nondenatured polyacrylamide gel at 10 °C.[29] As self-aggregation of purine-rich TFO sometimes competes with the triplex formation, TFO was used in this assay at low concentration such that no aggregation was observed. The triplex formation was performed by using a constant concentration of the TFO (10 nM) and different concentrations of the target duplex (0−100 nM), and the triplex was identified as the slower migrating band relative to the single-stranded TFO. Equilibrium association constants were obtained by quantification of the bands (Table 1).

Figure 5 illustrates the results of the electrophoresis with the use of the TFO incorporating WNA-7αG and -9αG. In the combinations of WNA-7αG/CG and 7αG/GC, triplex bands were observed at high concentrations of the target duplex (Figure 5A), indicating that WNA-7αG displayed lower binding constants with relative selectivity to a CG and a GC pair. In contrast, the TFO with WNA-9αG produced triplexes toward a TA pair selectively (Figure 5B). Compared with WNA-7βG,[18] it is interesting that the WNA-9αG exhibited higher potency in both selectivity and stability to a TA site. The WNA-A derivatives did not form stable triplexes, although some selectivity was observed in the combinations of WNA-βA/TA and WNA-αA/CG. As the triplexes with the WNA analogues connecting guanine or adenine were not satisfactorily stable compared with the natural triplexes (Z = dG, dA), we next investigated the WNA analogues bearing a pyrimidine base. To our surprise, WNA-βT exhibited a high stabilizing effect with selectivity to a TA base pair. It is also remarkable that selective stabilization of the triplex at a CG interrupting site has been achieved with WNA-βC. The WNA-pyrimidine analogues with α-stereochemistry did not produce a significant stabilizing effect. Triplex stability with WNA-βT analogues as well as with natural bases (dG and dA) could not be evaluated precisely, because the TFO was converted to the triplex even at low concentration of the target duplex. Therefore, we next examined triplex formation in a buffer containing 5 mM $MgCl_2$ instead of 20 mM $MgCl_2$ in the previous assay. The results of the gel-shift assay are shown in Figure 6, and the equilibrium association constants obtained from them are summarized in Table 2. Under the conditions with 5 mM $MgCl_2$, the TFO with WNA-βT yielded almost complete formation of a triplex with a TA interrupting site at a 10 nM duplex concentration (TFO/duplex = 1:1), whereas the other duplexes needed much higher concentrations for triplex formation (Figure 6A). Interestingly, the triplex with the WNA-βT/TA combination showed higher stability than the natural-type triplexes (Table 2). Furthermore, the association constant of the triplex with the WNA-βC/CG combination has been shown to be higher than that of the natural-type triplexes in the assay with 5 mM $MgCl_2$, although it was estimated to be less stable than the natural-type triplexes at 20 mM $MgCl_2$ (Table 1). The stability of the triplexes formed with WNA analogues is less affected by $MgCl_2$ concentration than that of natural-type triplexes. Consequently, it has been demonstrated that WNA-βT is a selective and high-affinity recognition motif to a TA interrupting site and that WNA-βC is a potential base analogue for a CG interrupting site.

To clarify the role of the benzene and thymine parts of WNA-βT, we evaluated the stability of the triplexes with the use of WNA-H (**7**) lacking a heterocyclic part and H-WNA-βT without a benzene ring (**8**) at a 5 mM $MgCl_2$ concentration. The TFO incorporating of WNA-H showed nonselective binding behavior with relatively higher affinity to CG and GC base pairs. It is apparent from these results that the bicyclic skeleton itself has a stabilizing effect for triplex formation. Surprisingly, the stability of the triplex containing WNA-H is higher than that

(24) Vorbrüggen H.; Krolikiewicz, K.; Bennua B. *Chem. Ber*. **1981**, *114*, 1234−1255.
(25) Vorbrüggen H.; Höfle, G. *Chem. Ber*. **1981**, *114*, 1256−1268.
(26) Garner, P.; Ramakanth, S. *J. Org. Chem.* **1988**, *53*, 1294−1298.
(27) Masköy, M.; Bolli, M.; Schweizer, B.; Leumann, C. J. *Helv. Chim. Acta* **1993**, *76*, 481−510.
(28) See the Supporting Information.
(29) Arimondo, P. B.; Barcelo, F.; Sun, J. S.; Maurizot, J. C.; Garestier, T.; Helene, C. *Biochemistry* **1998**, *37*, 16627−16635.

Scheme 2 [a]

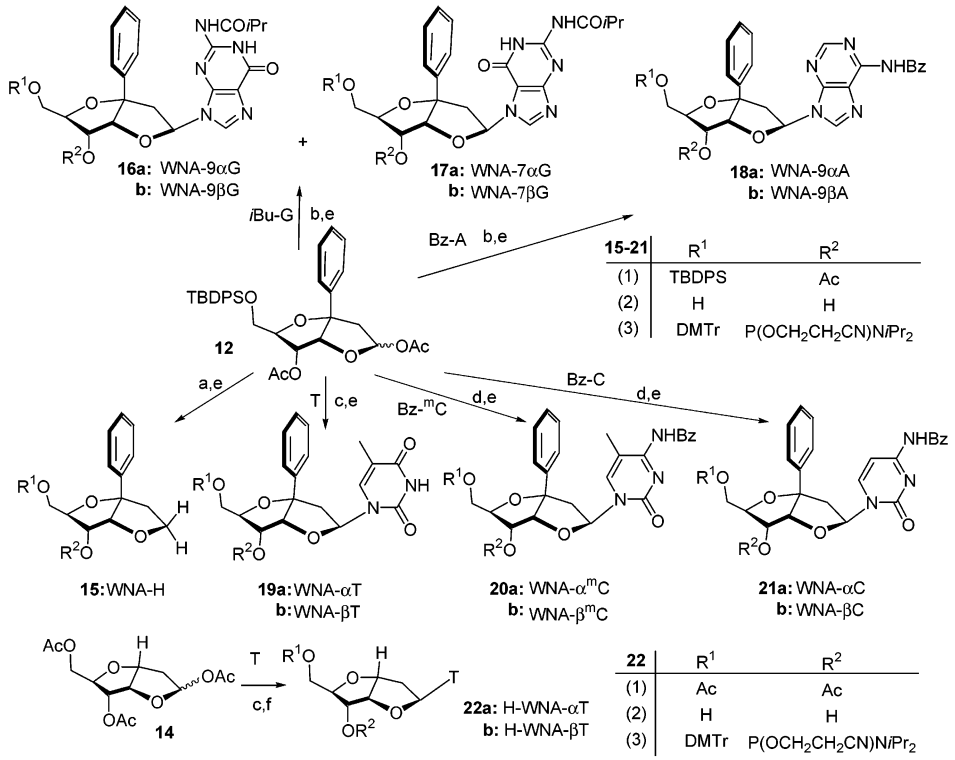

[a] (a) Et_3SiH, TMSOTf, CH_2Cl_2; (b) BSA, TMSOTf, CH_3CN; (c) HMDS, TMSCl, $SnCl_4$, CH_3CN; (d) BSA, $SnCl_4$,CH_3CN; (e) (i) $^nBu_4NF$, THF, (ii) aqueous NaOH, MeOH, (iii) DMTrCl, pyridine, (vi) iPr$_2$NP(Cl)OCH$_2$CH$_2$CN, iPr$_2$NEt, CH_2Cl_2; (f) (i) aqueous NaOH, MeOH, (ii) DMTrCl, pyridine, (iii) iPr$_2$NP(Cl)OCH$_2$CH$_2$CN, iPr$_2$NEt, CH_2Cl_2.

Table 1. Equilibrium Association Constants (K_s, 10^9 M^{-1}) of the Triplexes at 20 mM $MgCl_2$ Concentrations[a]

	X,Y			
Z	T,A	A,T	C,G	G,C
dG	0.16	0.08	0.09	>***1.0***
dA	0.069	>***1.0***	0.057	0.40
WNA-7βG	***0.02***	0.01	<0.001	<0.001
WNA-9βG	<0.001	***0.01***	<0.001	<0.001
WNA-7αG	<0.001	0.008	***0.023***	***0.021***
WNA-9αG	***0.10***	0.013	0.017	0.017
WNA-βA	***0.26***	0.015	0.063	0.029
WNA-αA	0.007	0.009	***0.067***	0.036
WNA-βT	>***1.0***	0.042	0.091	0.045
WNA-αT	0.009	<0.001	<0.001	<0.001
WNA-β^mC	***0.42***	0.018	0.03	0.029
WNA-α^mC	<0.001	<0.001	<0.001	<0.001
WNA-βC	0.057	0.032	***0.152***	0.055
WNA-αC	0.014	<0.001	0.017	0.023

[a] Triplex formation and gel-shift assay were performed as described for Figure 5, and the bands corresponding to the unbound TFO and the triplex were quantified. The equilibrium association constant was calculated by the equation K_s = [triplex]/([TFO][duplex]). Concentrations of each component represented as [triplex], [TFO], and [duplex] were estimated from the relative ratio of the bands.

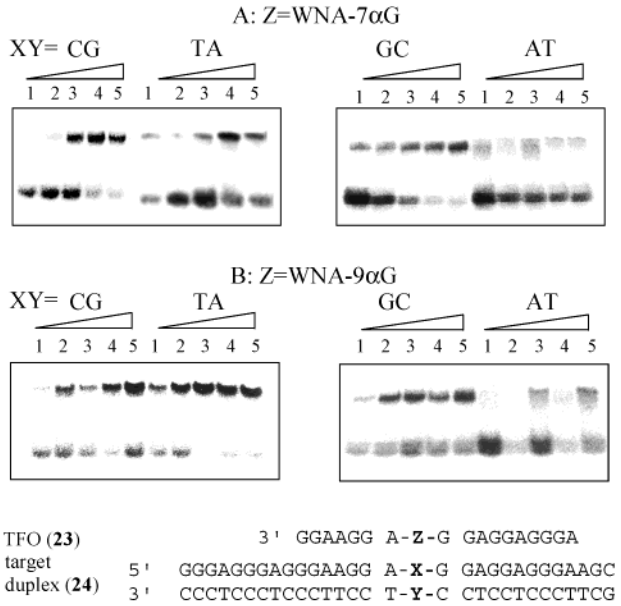

Figure 5. Gel-shift assay for determination of triplex formation with WNA-7αG and -9αG. Triplex formation was done for 12 h at 22 °C in a buffer containing 20 mM Tris-HCl, 20 mM $MgCl_2$, 2.5 mM spermidine, and 10% sucrose at pH 7.5. Electrophoresis was done at 10 °C with 20% nondenatured polyacrylamide gel. 10 nM TFO containing the ^{32}P-labeled one as the tracer was used. The concentration of the duplex was increased from lane 1 to 5 (10, 20, 40, 60, 80 nM).

of the corresponding natural triplex including the G/GC triplet. It has been revealed from comparison of association constants between WNA-βT and WNA-H that the thymine unit of WNA-βT causes a high stabilizing effect selectively to the TA site, whereas it leads to large destabilization in the other three combinations. On the other hand, in the case of WNA-βC, destabilization to the CG pair is less than that to the TA and the GC base pairs, resulting in selectivity to the CG pair. The fact that H-WNA-βT did not produce stable triplexes at any combination clearly suggests that the benzene ring brings about a major stabilizing effect with the WNA analogues.

We also examined the triplex-forming ability of WNA-βT to see whether it can stabilize a triplex containing the sequential

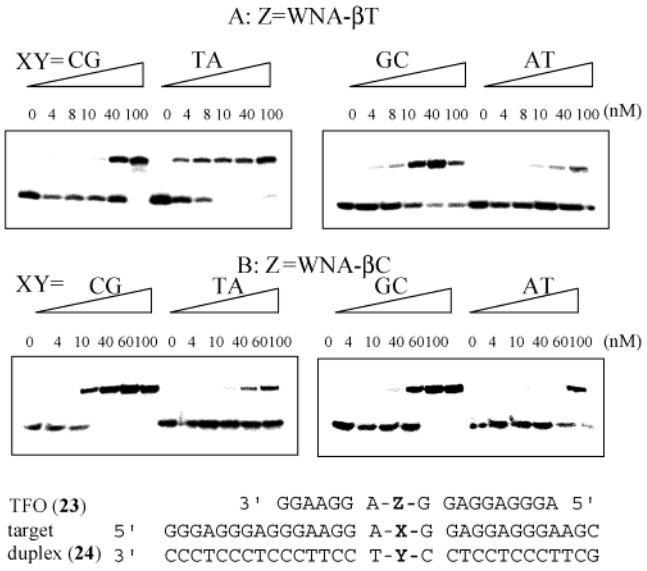

Figure 6. Gel-shift assay for determination of triplex formation. The conditions for triplex formation and gel-shift assay are the same as those for Figure 5 except for the use of the buffer containing 5 mM $MgCl_2$.

Table 2. Equilibrium Association Constants (K_s, 10^9 M^{-1}) of the Triplexes at 5 mM $MgCl_2$ Concentrations[a]

	X,Y			
Z	T,A	A,T	C,G	G,C
dG	0.004	0.008	0.008	**0.086**
dA	<0.001	**0.074**	<0.001	0.047
WNA-βT	**0.30**	<0.001	0.015	0.082
WNA-βC	<0.001	0.025	**0.115**	*0.047*
WNA-H	0.067	0.047	**0.18**	**0.28**
H-WNA-βT	0.002	0.003	0.009	0.042

[a] Triplex formation and gel-shift assay were performed as described for Figure 6, and the bands corresponding to the unbound TFO and the triplex were quantified. The equilibrium association constant was calculated by the equation K_s = [triplex]/([TFO][duplex]). Concentrations of each component represented as [triplex], [TFO], and [duplex] were estimated from the relative ratio of the bands.

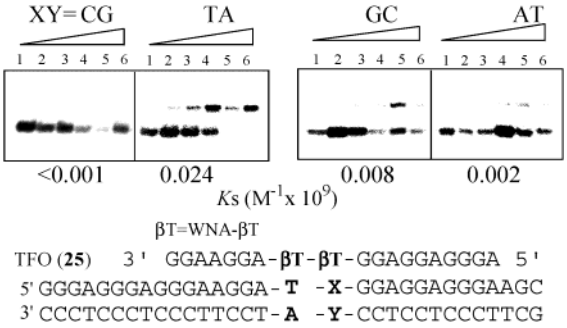

Figure 7. Triplex formation with the TFO incorporating two continuous WNA-βT analogues. The conditions for the triplex formation and gel-shit assay are the same as described for Figure 5. Concentrations of the duplex in lanes 1 to 6: 10, 20, 40, 60, 80, and 100 nM.

two TA interrupting sites or not (Figure 7). The gel-shift assay showed that the TFO (**25**) with two continuous WNA-βT units formed the triplex selectively with the target duplex with the sequential two TA interrupting sites. Although stability of the triplex formed with the TFO (**25**) is lower than that containing a single WNA-βT/TA combination (**23**), achievement of triplex formation with selectivity to two continuous TA interrupting sites is of potential significance in future development of new WNA analogues for further expansion of the target sequence.

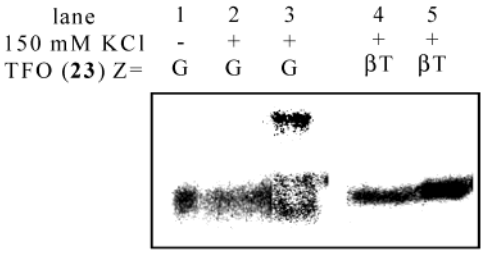

Figure 8. Gel-shift assay of the TFOs. TFOs were incubated under the conditions described in Figure 5 in the presence or absence of KCl. Electrophoresis was done at 10 °C with 15% nondenatured polyacrylamide gel. 10 nM TFO was used in lanes 1, 2, and 4, and 3 μM TFO was used in lanes 3 and 5.

A shortcoming of homopurine-TFOs in the formation of triplexes is that they tend to form self-aggregation in the presence of alkali metal cations to diminish the ability for triplex formation.[30] In the assay using 3 μM TFO concentration in the presence of 150 mM KCl, the natural-type TFO (**23**, Z = G) was observed to form higher molecular-weight bands that are suggestive of aggregation (Figure 8, lane 3). In a remarkable contrast, the TFO incorporating WNA-βT did not indicate aggregate formation under the same conditions (Figure 8, lane 5). These results have suggested another advantageous point of the WNA analogues in that they may be useful in application under physiological conditions.

Discussion

The new nucleoside analogues (WNA) have been designed based on our original concept of separating the hydrogen bonding and base-stacking contributors into two parts, and potential new compounds, WNA-βT (**4b**) for a TA and WNA-βC (**5b**) for a CG interrupting site, have been developed for selective stabilization of triplexes. As a matter of great interest, the triplex stability with WNA-H without a base unit is higher than that of the natural triplex (Table 2). It is apparent from comparison of the stabilizing effect of H-WNA-βT without benzene that benzene of WNA-H is a major contributor to triplex stability. As a benzene nucleotide has been shown to stack with slightly greater affinity than thymine in a duplex,[31,32] the stabilizing effect of a benzene of WNA-H might be also attributable to stacking interactions in the triplex. The five-membered ring between the 1′- and 2′-position might increase hydrophobicity of the WNA-H, resulting in additional stabilization of the triplex.[33] Based on the stabilizing effect of WNA-H, it is clear that the high selectivity of WNA-βT is brought about by the high stabilizing effect of thymine to a TA site together with its large destabilizing effect to the other base pairs (Table 2). In a similar context, selectivity of WNA-βC to a CG site may be explained in terms of differences in the destabilizing effect of cytosine to the base pairs. Factors for stabilization might include hydrogen bonds or van der Waals interactions to a favorable base pair, and destabilizing effects might be due to steric repulsions with unfavorable base pairs.

(30) Olivas, W. M.; Maher, L. J., III. *Nucleic Acids Res.* **1995**, *23*, 1936−1941.
(31) Guckian, K. M.; Schweitzer, B. A.; Ren, R. X.-F.; Sheils, C. J.; Paris, P. L.; Tahmassebi, D. C.; Kool, E. T. *J. Am. Chem. Soc.* **1996**, *118*, 8182−8183.
(32) Guckian, K. M.; Schweitzer, B. A.; Ren, R. X.-F.; Sheils, C. J.; Paris, P. L.; Tahmassebi, D. C.; Kool, E. T. *J. Am. Chem. Soc.* **2000**, *122*, 2213−2222.
(33) See p 217 in ref 1 for a discussion of contribution of hydrophobicity in triplex stabilization.

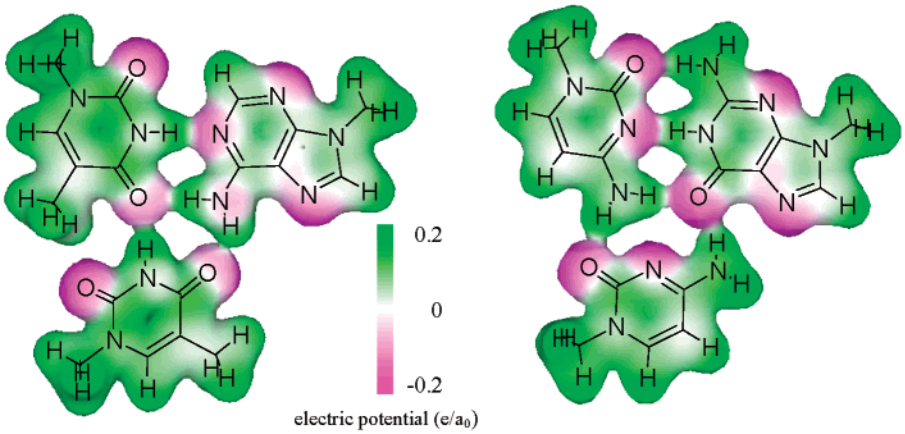

Figure 9. Speculated complex structures of thymine to a TA and cytosine to a CG base pair. These complex structures were optimized with PM3. Electric potentials were displayed by 3D mapped isosurface.

In the initial design of the WNA analogue, selective hydrogen bonds between the guanine and the distant adenine of the TA interrupting site were anticipated (Figure 1D). However, all the WNA isomers with guanine and adenine did not produce stable triplexes. In comparison with the stability of natural triplexes or that with WNA-H, purine bases of the WNA analogues act as destabilizing factors, probably because they might be repulsive to the backbone of the pyrimidine strand of the duplex.

Molecular modeling has suggested that the thymine of the WNA-βT might form hydrogen bonds to both bases of a TA base pair rather than Hoogsteen-type hydrogen bonds with the distant adenine. Similarly, hydrogen bonds of cytosine to both bases of a CG base pair might be also plausible. Figure 9 depicts such model triplets of T/TA and C/CG together with calculated 3D mapped isosurface of electric potential, presenting possible hydrogen bondings at the junction region. Lower stability of the triplex with WNA-β^{m}C for a CG site might be rationalized by assuming protonation at 3-*N* of 5-methycytosine. This assumption is supported in principle by the observation that the association constant of the triplex with a WNA-β^{m}C/CG is increased as the pH of buffer increased (relative ratio of the association constant at 5 mM $MgCl_2$ is 0.6 at pH 7.0, 1.0 at pH 7.5, and 1.9 at pH 8.0). In a complex structure determined for T/CG mismatched base triplet in the antiparallel triplex, hydrogen bonds of a water molecule between the guanine and thymine at the junction were postulated to produce stabilizing effect.[34,35] Detailed study is needed for understanding of the recognition mechanism of the WNA analogues.

Compared to the previous studies with limited success by the use of nucleoside analogues with 1′-α stereochemistry, the remarkable success of the WNA analogue with a bicyclo[3.3.0]-octane skeleton may be attributable to cooperative action of a benzene ring and a nucleobase unit. An advantageous property of WNA analogues showing resistance to self-aggregation may be due to steric disorder of the TFO caused by incorporating a WNA analogue. In the case of triplex formation by the TFO with two continuous WNA analogues, as triplex stability is diminished to a large extent, its steric factor might become a disadvantage. Detailed information on the structures of the triplexes with the WNA analogues, together with elucidation of the roles of each component, will be useful for the design of new WNA analogues to expand triplex recognition codes.

Conclusion

In this study, we have determined two new nucleoside analogues, WNA-βT (**4b**) and WNA-βC (**5b**), for the formation of stable triplexes with selectivity to a TA and a CG interrupting site, respectively. These useful properties are provided by cooperative work of a benzene ring and a nucleobase attached to the bicyclo[3.3.0]octane skeleton and are characteristic in that the stability of the triplexes with them is higher than that of natural-type triplexes in the presence of low Mg^{2+} concentration. Thus, the new WNA analogues might have a high potential for DNA recognition with TFOs in application to living systems. A future challenge is the development of new WNA analogues for expansion of triplex recognition codes to a general duplex sequence having continuous or random interrupting sites, and studies are now in progress along this line.

Experimental Section

General. ^{1}H NMR (270, 400, 500, or 600 MHz) and ^{13}C NMR (100, 125 MHz) spectra were recorded on a JEOL GX-270, Varian UNITY-400, INOVA-500, or INOVA-600 spectrometer. Infrared (IR) spectra were obtained using a SHIMADZU FTIR-8400 spectrometer. High-resolution mass spectra analyses were recorded on an Applied Biosystems Mariner System 5299 spectrometer using bradykinin, neurotensin, and angiotensin as an internal standard.

Synthesis. 5-*O*-*tert*-Butyldiphenylsilyl-2,3-*O*-isopropylidene-D-ribono-1,4-lactone 9. A suspension of D-ribose (42.4 g, 0.28 mol) and *p*-toluenesulfonic acid monohydrate (1.8 g, 9.6 mmol) in acetone (415 mL, 5.6 mol) was stirred for 20 h at room temperature. The reaction mixture was quenched with $NaHCO_3$ (1.2 g, 14.4 mmol), the solids were filtered off, and then the filtrate was evaporated. To a solution of the residue in CH_2Cl_2 (420 mL) at 0 °C were added Et_3N (39 mL, 0.28 mol), *tert*-butylchlorodiphenylsilane (72.8 mL, 0.28 mol), and DMAP (3.4 g, 0.028 mol). After stirring at room temperature for 1 h, the reaction mixture was diluted with EtOAc, and the organic layers were successively washed with sat. NH_4Cl solution, water, and brine, dried over Na_2SO_4, and evaporated. The residue was purified by flash chromatography (silica gel, hexane/EtOAc = 5:1) to give a colorless oil in 83%. A solution of this colorless oil (99 g, 0.23 mol) in CH_2Cl_2 (190 mL) was added to a suspension of Celite545 (230 g) and PCC (148.5 g, 0.69 mol) in CH_2Cl_2 (1.6 L). After stirring for 16 h at room temperature, the reaction mixture was diluted with EtO_2 and filtered through a Celite545 pad, and then the filtrate was evaporated. The residue was purified by flash chromatography (silica gel, hexane/EtOAc

(34) Dittrich, K.; Gu, J.; Tinder, R.; Hogan, M.; Gao, X. *Biochemistry* **1994**, *33*, 4111−4120.
(35) Floris, R.; Scaggiante, B.; Manzini1, G.; Quadrifoglio, F.; Xodo, L. E. *Eur. J. Biochem.* **1999**, *260*, 801−809.

= 1:1) to give **9** as white solids (75.8 g, 0.18 mol, 77%). Mp 96−97 °C. ^{1}H NMR (400 MHz, $CDCl_3$/TMS) δ 1.04 (s, 9H), 1.39 (s, 3H), 1.48 (s, 3H), 3.76 (d 1H, J = 11.42 Hz), 3.91 (d, 1H, J = 11.42 Hz), 4.57 (s, 1H), 4.73 (d, 1H, J = 5.61 Hz), 4.89 (d, 1H, J = 5.61 Hz), 7.39−7.48 (m, 6H), 7.62 (d, 2H, J = 6.36 Hz), 7.63 (d, 2H, J = 6.18 Hz). FTIR (film) 1790 cm^{-1}. HRMS (ESIMS) *m*/*z* calcd for $C_{24}H_{30}O_5$SiNa (M+Na)$^+$ 449.1755, found 449.1747. Anal. Calcd for $C_{24}H_{30}O_5$Si: C, 67.57; H, 7.09. Found: C, 67.87; H, 7.19.

(1*R*,5*R*,6*RS*,8*R*)-3,3-Dimethyl-6-phenyl-6-(2′-propenyl)-8-(*tert*-butyldiphenylsilyloxymethyl)-2,4,7-trioxabicyclo[3.3.0]octane 11. A solution of phenyllithium in cyclohexane−diethyl ether solution (1.04 M, 13.9 mL, 14.4 mmol) was added to a solution of **9** (4.1 g, 9.60 mmol) in THF (60 mL) at −78 °C in portions. After stirring for 2 h at −78 °C, the reaction mixture was allowed to warm to room temperature, quenched with sat. NH_4Cl solution, and extracted with EtOAc. The organic layer was successively washed with water and brine, dried over Na_2SO_4, and evaporated. The residue was purified by flash chromatography (silica gel, hexane/EtOAc = 7:1) to give **10** as a yellow oil (3.83 g, 79%). The solution of this colorless oil (3.83 g, 7.59 mmol) in CH_3NO_2 (10 mL) and allyltrimethylsilane (1.6 mL, 10.1 mmol) was added to a suspension of zinc bromide (4.91 g, 21.8 mmol) at 0 °C. After stirring for 2 h at room temperature, the reaction mixture was quenched with sat. $NaHCO_3$ and extracted with EtOAc. The organic layers were successively washed with water and brine, dried over Na_2SO_4, and then evaporated. The residue was purified by flash chromatography (silica gel, hexane/EtOAc = 19:1) to give **11** as a colorless oil (α-isomer/β-isomer = 1.8 g/1.5 g, 82%). α-isomer: ^{1}H NMR (270 MHz, $CDCl_3$/TMS) δ 1.02 (s, 9H), 1.37 (s, 3H), 1.63 (s, 3H), 2.59 (dd 1H, J = 6.9, 14.5 Hz), 2.79 (dd, 1H, J = 7.3, 14.5 Hz), 3.73 (dd, 1H, J = 5.0, 10.9 Hz), 3.80 (dd, 1H, J = 4.6, 10.9 Hz), 4.25 (dt, 1H, J = 3.3, 4.9 Hz), 4.67−4.75 (m, 2H), 4.86−4.89 (m, 1H), 4.92 (d, 1H, J = 1.7 Hz), 5.49−5.64 (m, 1H), 7.17−7.46 (m, 11H), 7.63−7.69 (m, 4H). FTIR (film) 1640, 1420 cm^{-1}. HRMS (ESIMS) *m*/*z* calcd for $C_{33}H_{40}O_4$SiNa (M + Na)$^+$ 551.2588, found 551.2602.

(1*R*,3*R*,4*R*,5*R*,7*RS*)-1-Phenyl-3-(*tert*-butyldiphenylsilyloxymethyl)-4,7-diacetoxy-2,6-dioxabicyclo[3.3.0]octane 12. Aqueous solutions of OsO_4 (0.131 M, 2.0 mL, 0.262 mmol) and $NaIO_4$ (0.6 M, 10 mL, 6.0 mmol) were added to a solution of **11** (1.03 g, 1.59 mmol) in pyridine (13 mL), and the reaction mixture was stirred for 30 h at room temperature. The reaction mixture was diluted with EtOAc and successively washed with water and brine, dried over Na_2SO_4, and evaporated. A solution of the residue in THF (20 mL)/5% H_2SO_4 (4 mL) was stirred for 6 h at 60 °C, quenched by the addition of sat. $NaHCO_3$ solution, and extracted with EtOAc. The organic layer was successively washed with water and brine, dried over Na_2SO_4, and evaporated. The residue was purified by flash chromatography (silica gel, $CHCl_3$/EtOAc = 2:1) to give a colorless foam (269 mg, 28%, for two steps). Acetic anhydride (0.45 mL, 4.76 mmol) was added to a solution of the colorless foam (585 mg, 1.19 mmol) in pyridine (6 mL) at 0 °C and stirred for 39 h at room temperature. The reaction mixture was diluted with EtOAc and successively washed with water and brine, dried over Na_2SO_4, and evaporated. The residue was purified by flash chromatography (silica gel, hexane/EtOAc = 5:1) to give **12** as a colorless foam (613 mg, 90%). ^{1}H NMR (500 MHz, $CDCl_3$) δ 1.05 (s, 9H), 2.03 (s, 3H), 2.14 (s, 3H), 2.65 (dd 1H, J = 1.83, 15.1 Hz), 2.86 (dd, 1H, J = 5.95, 15.1 Hz), 3.76 (dd, 1H, J = 3.44, 11.68 Hz), 4.06 (dd, 1H, J = 2.75, 11.68 Hz), 4.22 (dt, 1H, J = 2.98, 9.38 Hz), 4.83 (d, 1H, J = 4.12 Hz), 5.05 (dd, 1H, J = 4.12, 9.38 Hz), 6.62 (dd, 1H, J = 1.83, 5.95 Hz), 7.27−7.45 (m, 9H), 7.63−7.71 (m, 6H). FTIR (film) 1740, 1370, 1230 cm^{-1}. HRMS (ESIMS) *m*/*z* calcd for $C_{33}H_{38}O_7$SiNa (M + Na)$^+$ 597.2279, found 597.2256.

(1*R*,5*R*,6*R*,8*R*)-8-Acetoxymethyl-3,3-dimethyl-6-(2′-propenyl)-2,4,7-trioxabicyclo[3.3.0]octane 13. Trityl perchlorate (1.8 g, 5.3 mmol) was added to a solution of 1,5-*O*-diacetyl-2,3-*O*-isopropylidene-D-ribose (14.6 g, 53.2 mmol) and allyltrimethylsilane (22.9 mL, 144 mmol) in 1,2-dimethoxyethane (292 mL) at 0 °C. The reaction mixture was stirred for 3 h at room temperature, diluted with 10 mM phosphate buffer (pH7), and extracted with ether. The organic layer was washed with brine, dried over $MgSO_4$, then evaporated. The residue was purified by flash chromatography (silica gel, hexane/EtOAc = 5:1) to give **13** as a colorless oil (9.18 g, 79%). ^{1}H NMR (400 MHz, $CDCl_3$): δ 1.34 (s, 3H), 1.54 (s, 3H), 2.10 (s, 3H), 2.34−2.38 (m, 2H), 4.00 (dd, 1H, J = 6.18, 10.9 Hz), 4.08−4.14 (m, 2H), 4.25−4.30 (m, 1H), 4.39 (dd, 1H, J = 4.30, 6.74 Hz), 4.49 (dd, 1H, J = 4.30, 6.79 Hz), 5.12−5.18 (m, 2H), 5.77−5.87 (m, 1H). FTIR ($CHCl_3$) 1740 cm^{-1}. HRMS (ESIMS) *m*/*z* calcd for $C_{13}H_{20}O_5$Na (M + Na)$^+$ 279.1203, found 279.1172.

(1*R*,3*R*,4*R*,5*S*,7*RS*)-3-Acetoxymethyl-4,7-diacetoxy-2,6-dioxabicyclo-[3.3.0]octane 14. Aqueous solutions of OsO_4 (0.131 M, 83.8 mL, 11 mmol) and $NaIO_4$ (0.6 M, 343 mL, 206 mmol) were added to a solution of **13** (9.1 g, 34.3 mmol) in pyridine (168 mL), and the mixture was stirred for 2 h at room temperature. The reaction mixture was diluted with EtOAc and successively washed with water and brine, dried over Na_2SO_4, and evaporated. The residue was purified by flash chromatography (silica gel, hexane/EtOAc = 3:1) to give a pale yellow oil (5.96 g, 65%). A solution of this oil in 2 M HCl solution (36.5 mL) and THF (183 mL) was stirred for 1 h at 40 °C. The reaction mixture was neutralized with Et_3N (10 mL), diluted with EtOAc, successively washed with sat. $NaHCO_3$ solution, water, and brine, and dried over Na_2SO_4, then evaporated. The residue was purified by flash chromatography (silica gel, $CHCl_3$/MeOH = 30:1) to give a bicyclic compound as a pale yellow oil (3.47 g, 69%). A solution of the above product (3.0 g, 13.7 mmol) and acetic anhydride (5.1 mL, 55.2 mmol) in pyridine (120 mL) was stirred for 30 min at 0 °C and for 2 h at room temperature. The reaction mixture was diluted with EtOAc and successively washed with 10% HCl solution, brine, sat. $NaHCO_3$ solution, and brine. The organic layer was dried over Na_2SO_4 and evaporated. The residue was purified by flash chromatography (silica gel, hexane/EtOAc = 5:1) to give **14** as a colorless oil (2.4 g, 58%). ^{1}H NMR (400 MHz, $CDCl_3$): δ 2.01 (s, 3H), 2.07 (s, 3H), 2.11 (s, 3H), 2.35 (t, 2H, J = 3.93 Hz), 4.05−4.13 (m, 2H), 4.30−4.33 (m, 1H), 4.81−4.87 (m, 2H), 4.93 (dd, 1H, J = 4.68, 9.36 Hz), 6.46 (t, 1H, J = 4.11 Hz). FTIR ($CHCl_3$) 1743 cm^{-1}. ESIMS (*m*/*z*): 325 (M + Na)$^+$.

(1*S*,3*R*,4*R*,5*R*)-4-Acetoxy-1-phenyl-3-(*tert*-butyldiphenylsilyloxymethyl)-2,6-dioxabicyclo[3.3.0]octane, WNA-H, 15(1). Et_3SiH (810 mg, 7.7 mmol) was added to a solution of **12** (400 mg, 0.7 mmol) in CH_2Cl_2 (7 mL) at room temperature under argon, and the reaction mixture was stirred at room temperature for 15 min, then cooled to 0 °C, followed by the addition of $CF_3SO_3SiMe_3$ (0.317 mL, 1.75 mmol). After stirring for 1 h at 0 °C, the mixture was diluted with sat. $NaHCO_3$ solution and extracted with AcOEt. The organic layer was successively washed with water and brine, dried over Na_2SO_4, and evaporated. The residue was purified by flash chromatography (silica gel, hexane/AcOEt = 10:1) to give WNA-H (**15(1)**) as a colorless oil (294 mg, 81%). ^{1}H NMR (270 MHz, $CDCl_3$/TMS) δ 1.02 (s, 9H), 2.06 (s, 3H), 2.40−2.57 (m, 2H), 3.73 (dd, 1H, J = 3.63, 11.54 Hz), 4.01 (dd, 1H, J = 3.30, 11.55 Hz), 4.09 (dt, 1H, J = 6.27, 8.91 Hz), 4.15−4.26 (m, 2H), 4.66 (d, 1H, J = 4.29 Hz), 5.08 (dd, 1H, J = 4.61, 9.23 Hz), 7.21−7.70 (m, 15H). FTIR ($CHCl_3$) 1740 cm^{-1}. HRMS (ESIMS) *m*/*z* calcd for $C_{31}H_{36}O_5$SiNa (M + Na)$^+$ 539.2224, found 539.2240.

Glycosidation. The synthesis of **16(1)** and **17(1)** was described as a general procedure. The compounds (**19**−**22**) were synthesized in a similar manner except for the reagents used.

(1′*S*,3′*R*,4′*R*,5′*R*,7′*S* and 7′*R*)-*N*^{2}-Isobutyryl-9-and-7-{4′-acetoxy-1′-phenyl-3′-(*tert*-butyldiphenylsilyloxymethyl)-2′,6′-dioxabicyclo-[3.3.0]oct-7′-yl}guanine, WNA-9α,*β*G and -7α,*β*G, 16a,b(1) and 17a,b(1). *N*,*O*-Bis(trimethylsilyl)acetamide (BSA; 500 mL, 1.97 mmol) was added to a suspension of *N*^{2}-isobutyrylguanine (71 mg, 0.321 mmol) in CH_3CN (25 mL) at 50 °C. A solution of TMSOTf (30 mL, 0.166 mmol) and **12** (166 mg, 0.289 mmol) in CH_3CN (1.0 mL) was added to the above mixture. The reaction mixture was stirred at 50 °C

for 4 h and diluted with MeOH and evaporated. A solution of the above residue in EtOAc was successively washed with sat. $NaHCO_3$, water, and brine, dried over Na_2SO_4, and evaporated. The isomers were separated by flash chromatography (silica gel, acetone/hexane = 1:2) to give each isomer in total 88% yield. WNA-9αG (**16a(1)**): a white powder (80 mg, 38%). Mp 122−125 °C. ^{1}H NMR (500 MHz, $CDCl_3$) δ 0.99 (s, 9H), 1.26 (d, 6H, J = 6.9 Hz), 1.94 (s, 3H), 2.55 (pseudoquintet, 1H, J = 6.9 Hz), 3.04 (dd, 1H, J = 7.9, 15.2 Hz), 3.16 (dd, 1H, J = 4.3, 15.0 Hz), 3.67 (dd, 1H, J = 3.6, 11.8 Hz), 3.93 (dd, 1H, J = 3.0, 11.5 Hz), 4.10 (ddd, 1H, J = 3.0, 3.6, 8.2 Hz), 4.97 (d, 1H, J = 4.0 Hz), 5.07 (dd, 1H, J = 4.0, 8.6 Hz), 6.42 (dd, 1H, J = 4.0, 7.9 Hz), 7.30−7.44 (m, 9H), 7.55−7.64 (m, 6H), 8.15 (bs, 1H), 8.20 (s, 1H), 12.0 (bs, 1H). FTIR ($CHCl_3$) 1740, 1690 cm^{-1}. FABMS (*m*/*z*) 736 (M + H)$^+$. WNA-9β**G** (**16b(1)**): a white powder (32 mg, 15%). Mp 120−125 °C. ^{1}H NMR (500 MHz, $CDCl_3$) δ 1.01 (s, 9H), 1.29 (d, 6H, J = 6.9 Hz), 2.02 (s, 3H), 2.59 (pseudoquintet, 1H, J = 6.9 Hz), 3.01 (dd, 1H, J = 6.6, 14.3 Hz), 3.08 (dd, 1H, J = 7.7, 14.3 Hz), 3.75 (dd, 1H, J = 3.6, 11.5 Hz), 4.01 (dd, 1H, J = 3.0, 11.5 Hz), 4.31 (dt, 1H, J = 3.3, 9.1 Hz), 5.14 (dd, 1H, J = 3.8, 9.1 Hz), 5.22 (d, 1H, J = 3.6 Hz), 6.30 (dd, 1H, J = 6.9, 7.4 Hz), 7.27−7.45 (m, 9H), 7.60−7.66 (m, 6H), 7.82 (s, 1H), 7.88 (bs, 1H), 11.9 (bs, 1H). FTIR ($CHCl_3$) 1740, 1690 cm^{-1}. FABMS (*m*/*z*): 736 (M + H)$^+$. HRMS (FABMS) *m*/*z* calcd for $C_{40}H_{46}N_5O_7Si$ (M + H)$^+$ 736.3175, found 736.3166. WNA-7αG (**17a(1)**): a white powder (54 mg, 25%). Mp 122−124 °C. ^{1}H NMR (500 MHz, $CDCl_3$) δ 0.98 (s, 9H), 1.26 (d, 6H, J = 7.1 Hz), 1.93 (s, 3H), 2.55 (pseudoquintet, 1H, J = 7.1 Hz), 3.02 (dd, 1H, J = 8.0, 15.1 Hz), 3.02 (dd, 1H, J = 8.0, 15.1 Hz), 3.67 (dd, 1H, J = 3.9, 11.5 Hz), 3.92 (dd, 1H, J = 3.3, 11.5 Hz), 4.10 (ddd, 1H, J = 3.3, 3.6, 8.2 Hz), 4.96 (d, 1H, J = 3.9 Hz), 5.05 (dd, 1H, J = 3.9, 8.5 Hz), 6.40 (dd, 1H, J = 3.6, 8.0 Hz), 7.27−7.45 (m, 9H), 7.05−7.61 (m, 6H), 8.43 (s, 1H), 8.79 (bs, 1H), 12.1 (bs, 1H). FTIR ($CHCl_3$): 1740, 1690 cm^{-1}. FABMS (*m*/*z*): 736 (M + H)$^+$. WNA-7β**G** (**17b(1)**): a white powder (22 mg, 10%). Mp 122−125 °C. ^{1}H NMR (500 MHz, $CDCl_3$) δ 1.01 (s, 9H), 1.25 (d, 6H, J = 6.9 Hz), 1.99 (s, 3H), 2.69 (pseudoquintet, 1H, J = 6.9 Hz), 2.94 (dd, 1H, J = 5.8, 13.7 Hz), 3.16 (dd, 1H, J = 8.5, 13.7 Hz), 3.78 (dd, 1H, J = 4.1, 11.5 Hz), 4.00 (dd, 1H, J = 3.3, 11.5 Hz), 4.29 (ddd, 1H, J = 3.6, 3.9, 8.8 Hz), 5.11 (dd, 1H, J = 3.6, 9.1 Hz), 5.34 (d, 1H, J = 3.6 Hz), 6.39 (dd, 1H, J = 5.8, 8.2 Hz), 7.26−7.45 (m, 9H), 7.63−7.73 (m, 6H), 8.01 (s, 1H), 9.25 (bs, 1H), 12.2 (bs, 1H). FTIR ($CHCl_3$) 1740, 1690 cm^{-1}. FABMS (*m*/*z*) 736 (M + H)$^+$.

(1′*S*,3′*R*,4′*R*,5′*R*,7′*S* and 7′*R*)-*N*^{6}-Benzoyl-9-{4′-acetoxy-1′-phenyl-3′-(*tert*-butyldiphenylsilyloxymethyl)-2′,6′-dioxabicyclo[3.3.0]oct-7′-yl}adenine, WNA-α and -βA, 18a,b(1). Reagents: *N*^{6}-Benzoyladenine (540 mg, 2.26 mmol), BSA (1.1 mL, 4.52 mmol), TMSOTf (29 μL, 0.16 mmol), **12** (650 mg, 1.13 mmol). WNA-αA (**18a(1)**): a white powder (129 mg, 15%). Mp 104−106 °C. ^{1}H NMR (500 MHz, $CDCl_3$): δ 0.98 (s, 9H), 2.02 (s, 3H), 3.12 (dd, 1H, J = 8.01, 15.11 Hz), 3.27 (dd, 1H, J = 3.66, 15.11 Hz), 3.68 (dd, 1H, J = 4.12, 11.67 Hz), 3.90 (dd, 1H, J = 3.66, 11.67 Hz), 4.13−4.15 (m, 1H), 5.03 (d, 1H, J = 4.12 Hz), 5.07 (dd, 1H, J = 4.12, 8.47 Hz), 6.74 (dd, 1H, J = 3.67, 8.01 Hz), 7.29−7.40 (m, 9H), 7.50−7.62 (m, 9H), 8.01 (d, 2H, J = 7.09 Hz), 8.55 (s, 1H), 8.82 (s, 1H), 8.92 (bs, 1H). FTIR (KBr): 1747, 1699, 1609, 1582 cm^{-1}. ESIMS (*m*/*z*): 776 (M + Na)$^+$. WNA-β**A** (**18b(1)**): a white powder (237 mg, 28%). Mp 102−105 °C. ^{1}H NMR (500 MHz, $CDCl_3$) δ 1.07 (s, 9H), 2.05 (s, 3H), 3.09 (dd, 1H, J = 6.18, 14.19 Hz), 3.47 (dd, 1H, J = 8.24, 14.19 Hz), 3.84 (dd, 1H, J = 4.12, 11.45 Hz), 4.07 (dd, 1H, J = 3.2, 11.45 Hz), 4.41 (dt, 1H, J = 3.66, 8.92 Hz), 5.16 (dd, 1H, J = 3.89, 8.92 Hz), 5.16 (dd, 1H, J = 3.66, 8.92 Hz), 5.34 (d, 1H, J = 3.89 Hz), 6.56 (dd, 1H, J = 6.18, 8.02 Hz), 7.28−7.79 (m, 18H), 8.06 (d, 2H, J = 7.09 Hz), 8.19 (s, 1H), 8.91 (s, 1H), 9.00 (bs, 1H). FTIR (KBr) 1747, 1699, 1609, 1582 cm^{-1}. ESIMS (*m*/*z*) 754 (M + H)$^+$.

(1′*S*,3′*R*,4′*R*,5′*R*,7′*S* and 7′*R*)-{4′-Acetoxy-1′-phenyl-3′-(*tert*-butyldiphenylsilyloxymethyl)-2′,6′-dioxabicyclo[3.3.0]oct-7′-yl}-thymine, WNA-α and -βT, 19a, b(1). Reagents: $(Me_3Si)_2NH$ (35.5 mg, 0.22 mmol), Me_3SiCl (23.9 mg, 0.22 mmol), $SnCl_4$ (84.4 mg, 0.324 mmol), thymine (37.4 mg, 0.275 mmol), **12** (155 mg, 0.27 mmol), CH_3CN (2 mL). WNA-αT (**19a(1)**): a colorless foam (64.9 mg, 37%). ^{1}H NMR (500 MHz, $CDCl_3$/TMS) δ 1.01 (s, 9H), 1.95 (s, 3H), 2.02 (s, 3H), 2.61 (dd, 1H, J = 5.72, 15.33 Hz), 2.86 (dd, 1H, J = 8.01, 15.33 Hz), 3.77 (dd, 1H, J = 4.81, 11.44 Hz), 3.91 (dd, 1H, J = 3.66, 11.44 Hz), 4.33 (dd, 1H, J = 4.35, 8.01 Hz), 4.80 (dt, 1H, J = 3.89 Hz), 4.99 (dd, 1H, J = 8.70, 4.12 Hz), 6.53 (dd, 1H, J = 5.72, 8.00 Hz), 7.25−7.46 (m, 10H), 7.60−7.65 (m, 6H), 8.04 (bs, 1H). FTIR (film): 3018, 1691 cm^{-1}. HRMS (ESIMS) *m*/*z* calcd for $C_{36}H_{40}N_2O_7SiNa$ (M + Na)$^+$ 663.2497, found 663.2544. WNA-β**T** (**19b(1)**): a colorless foam (72.3 mg, 42%). ^{1}H NMR (500 MHz, $CDCl_3$/TMS) δ 1.00 (s, 9H), 1.96 (s, 3H), 2.03 (s, 3H), 2.52 (dd, 1H, J = 8.69, 13.95 Hz), 2.88 (dd, 1H, J = 5.95, 13.95 Hz), 3.73 (dd, 1H, J = 3.43, 11.67 Hz), 3.98 (dd, 1H, J = 2.97, 11.67 Hz), 4.25 (dd, 1H, J = 3.43, 8.92 Hz), 5.06 (dd, 1H, J = 4.12, 8.92 Hz), 5.11 (d, 1H, J = 4.12 Hz), 6.31 (dd, 1H, J = 5.95, 8.69 Hz), 7.19−7.44 (m, 10H), 7.54−7.65 (m, 6H), 8.29 (bs, 1H). FTIR (film) cm^{-1} 3018, 1691. HRMS (ESIMS) *m*/*z* calcd for $C_{36}H_{40}N_2O_7SiNa$ (M + Na)$^+$ 663.2497, found 663.2456.

(1′*S*,3′*R*,4′*R*,5′*R*,7′*S* and 7′*R*)-*N*^{4}-Benzoyl-1-{4′-acetoxy-1′-phenyl-3′-(*tert*-butyldiphenylsilyloxymethyl)-2′,6′-dioxabicyclo[3.3.0]oct-7′-yl}-5-methylcytosine, WNA-α and -β^{m}C, 20a,b(1). Reagents: *N*^{4}-Benzoyl-cytosine (222.7 mg, 0.975 mmol), BSA (0.488 mL, 2.03 mmol), $SnCl_4$ (0.303 mL, 2.63 mmol), **12** (465 mg, 0.81 mmol). WNA-α^{m}C (**20a(1)**): a colorless foam (85.7 mg, 14%). ^{1}H NMR (270 MHz, $CDCl_3$/TMS) δ 1.03 (s, 9H), 2.06 (s, 3H), 2.19 (s, 3H), 2.68 (dd, 1H, J = 4.95, 15.18 Hz), 2.94 (dd, 1H, J = 7.92, 15.18 Hz), 3.77 (dd, 1H, J = 2.97, 11.55 Hz), 3.90 (dd, 1H, J = 3.63, 11.55 Hz), 4.34 (dd, 1H, J = 3.96, 8.24 Hz), 4.88 (d, 1H, J = 4.29 Hz), 5.03 (dd, 1H, J = 4.29, 8.25 Hz), 6.55 (dd, 1H, J = 5.29, 7.29 Hz), 7.28−7.73 (m, 18H), 7.85 (s, 1H), 8.33 (d, 2H, J = 6.93 Hz). FTIR ($CHCl_3$) 1707, 1572 cm^{-1}. HRMS (ESIMS) *m*/*z* calcd for $C_{43}H_{46}N_3O_7Si$ (M + H)$^+$ 744.3100, found 744.3112. WNA-β^m**C** (**20b(1)**): a pale yellow foam (317.7 mg, 53%). ^{1}H NMR (270 MHz, $CDCl_3$/TMS) δ 1.01 (s, 9H), 2.05 (s, 3H), 2.16 (s, 3H), 2.54 (dd, 1H, J = 8.58, 13.86 Hz), 2.97 (dd, 1H, J = 5.61, 13.86 Hz), 3.75 (dd, 1H, J = 3.63, 11.55 Hz), 4.01 (dd, 1H, J = 2.97, 11.55 Hz), 4.26 (dd, 1H, J = 5.61, 8.91 Hz), 5.08 (dd, 1H, J = 3.96, 8.91 Hz), 5.15 (d, 1H, J = 3.96 Hz), 6.36 (dd, 1H, J = 5.6, 8.58 Hz), 7.18−7.72 (m, 18H), 8.32 (d, 2H, J = 6.93 Hz). FTIR ($CHCl_3$) 1707, 1570 cm^{-1}. HRMS (ESIMS) *m*/*z* calcd for $C_{43}H_{46}N_3O_7Si$ (M + H)$^+$ 744.3100, found 744.3128.

(1′*S*,3′*R*,4′*R*,5′*R*,7′*S* and 7′*R*)-*N*^{4}-Benzoyl-1-{4′-Acetoxy-1′-phenyl-3′-(*tert*-butyldiphenylsilyloxymethyl)-2′,6′-dioxabicyclo[3.3.0]oct-7′-yl}cytosine, WNA-α and -βC, 21a,b(1). Reagents: BSA (0.95 mL, 3.92 mmol), **12** (900 mg, 1.57 mmol) in 8 mL of CH_3CN, *N*^{4}-benzoylcytosine (421 mg, 1.96 mmol) in 10 mL of CH_3CN, $SnCl_4$ (0.36 mL, 5.49 mmol). WNA-αC (**21a(1)**): a colorless foam (458.7 mg, 40%). ^{1}H NMR (270 MHz, $CDCl_3$/TMS) δ 1.02 (s, 9H), 2.06 (s, 3H), 2.71 (dd, 1H, J = 4.95, 15.34 Hz), 3.10 (dd, 1H, J = 7.26, 15.34 Hz), 3.75 (dd, 1H, J = 4.29, 11.31 Hz), 3.82 (dd, 1H, J = 4.29, 11.31 Hz), 4.24 (dt, 1H, J = 4.29, 8.08 Hz), 5.00 (d, 1H, J = 4.62 Hz), 5.08 (dd, 1H, J = 4.62, 8.08 Hz), 6.41 (dd, 1H, J = 4.95, 7.26 Hz), 7.27−7.70 (m, 19H), 7.93 (d, 2H, J = 7.26 Hz), 8.27 (d, 1H, J = 7.26 Hz). FTIR (KBr) 3071, 2930, 1746, 1666, 1485 cm^{-1}. HRMS (ESIMS) *m*/*z* calcd for $C_{42}H_{44}N_3O_7Si$ (M + H)$^+$ 730.2943, found 730.2977. WNA-β**C** (**21b-(1)**): a colorless foam (602.5 mg, 53%). ^{1}H NMR (270 MHz, $CDCl_3$/TMS) δ 1.02 (s, 9H), 2.06 (s, 3H), 2.52 (dd, 1H, J = 7.43, 14.35 Hz), 3.24 (dd, 1H, J = 6.10, 14.35 Hz), 3.76 (dd, 1H, J = 3.47, 11.71 Hz), 4.03 (dd, 1H, J = 2.81, 11.71 Hz), 4.29 (ddd, 1H, J = 2.81, 3.47, 9.07 Hz), 5.09 (dd, 1H, J = 4.29, 9.07 Hz), 5.18 (d, 1H, J = 4.29 Hz), 6.38 (dd, 1H, J = 6.10, 7.43 Hz), 7.27−7.71 (m, 19H), 7.94 (d, 2H, J = 7.26 Hz), 8.01 (d, 1H, J = 7.59 Hz). FTIR (KBr) 3069, 2930, 1747, 1665, 1485 cm^{-1}. HRMS (ESIMS): *m*/*z* calcd for $C_{42}H_{44}N_3O_7Si$ (M + H)$^+$ 730.2943, found 730.2919.

(1′*R*,3′*R*,4′*R*,5′*S*,7′*S* and 7′*R*)-{4′-Acetoxy-3′-acetoxymethyl-2′,6′-dioxabicyclo[3.3.0]oct-7′-yl}thymine, H-WNA-αT and WNA-βT,

22a,b(1). Reagents: $(Me_3Si)_2NH$ (192 mg, 1.19 mmol), Me_3SiCl (129 mg, 1.19 mmol), $SnCl_4$ (466 mg, 1.79 mmol), thymine (207 mg, 1.64 mmol), **14** (450 mg, 1.49 mmol), CH_3CN (40 mL). H-WNA-αT (**22a-(1)**): a colorless oil (29%): ^{1}H NMR (500 MHz, $CDCl_3$) δ 1.91 (s, 3H), 2.08 (s, 3H), 2.12 (s, 3H), 2.14−2.22 (m, 1H), 2.60 (dd, 1H, J = 6.18, 14.2 Hz), 4.08 (dd, 1H, J = 5.27, 11.9 Hz), 2.16 (ddd, 1H, J = 2.51, 5.27, 8.02 Hz), 4.28−4.32 (m, 1H), 4.87 (dd, 1H, J = 4.80, 7.79 Hz), 4.94 (t, 1H, J = 5.04 Hz), 5.04 (t, 1H, J = 4.58 Hz), 6.18 (dd, 1H, J = 6.41, 7.56 Hz), 7.01 (d, 1H, J = 1.14 Hz), 8.53 (bs, 1H). FTIR ($CHCl_3$) 3390, 1744, 1693 cm^{-1}. HRMS (ESIMS) m/z calcd for $C_{16}H_{21}N_2O_8$ $(M + H)^+$ 369.1292, found 369.1327. H-WNA-βT (**22b-(1)**): a colorless oil (46%). ^{1}H NMR (500 MHz, $CDCl_3$) δ 1.86 (s, 3H), 2.08 (s, 3H), 2.09 (s, 3H), 2.44 (dd, 1H, J = 8.70, 14.2 Hz), 2.77−2.82 (m, 1H), 4.08 (dd, 1H, J = 5.50, 11.7 Hz), 4.10−4.13 (m, 1H), 4.32 (dd, 1H, J = 2.29, 11.7 Hz), 4.82 (dd, 1H, J = 4.58, 8.47 Hz), 5.10 (d, 2H, J = 5.49 Hz), 6.91 (d, 1H, J = 4.81 Hz), 6.92 (d, 1H, J = 5.27 Hz), 8.71 (bs, 1H). FTIR ($CHCl_3$) 3427, 1740, 1720, 1659 cm^{-1}. HRMS (ESIMS) m/z calcd for $C_{16}H_{20}N_2O_8Na$ $(M + Na)^+$ 391.1112, found 391.1071.

Deprotection: General Procedure. A THF solution of the above compound and TBAF (1.0 M THF solution, 2 equiv) was stirred for 1−2 h at room temperature, and the reaction mixture was diluted with AcOEt. The organic layer was successively washed with water and brine, dried over Na_2SO_4, and evaporated. The residue was purified by flash chromatography (silica gel, $CHCl_3$−CH_3OH) to give the corresponding compound, which was further deacetylated in a solution of THF/methanol = 9:1 containing 0.2 M NaOH (2 equiv) at 0 °C. After stirring for 45−60 min at 0 °C, the reaction mixture was quenched with acetic acid and diluted with MeOH, and then the solvent was evaporated. The residue was purified by flash chromatography (silica gel, $CHCl_3$−CH_3OH).

(1*S*,3*R*,4*R*,5*R*)-4-Hydroxy-3-hydroxymethyl-1-phenyl-2,6-dioxabicyclo[3.3.0]octane, **WNA-H, 15(2).** A white powder (70%). mp 122−125 °C. ^{1}H NMR (400 MHz, CD_3OD) δ 2.36 (ddd, 1H, J = 3.18, 5.99, 13.1 Hz), 2.50 (ddd, 1H, J = 8.24, 9.73, 13.1 Hz), 3.83−3.94 (m, 3H), 4.09 (ddd, 1H, J = 5.99, 8.62, 9.73 Hz), 4.23 (dt, 1H, J = 3.0, 8.24 Hz), 4.29 (d, 1H, J = 4.11 Hz), 7.23 (t, 1H, J = 7.49 Hz), 7.33 (t, 2H, J = 7.49 Hz), 7.55 (d, 2H, J = 7.49 Hz). ^{13}C NMR (100 MHz, CD_3OD): δ 45.43, 63.65, 71.32, 73.67, 84.82, 90.25, 94.07, 126.23, 128.14, 129.22, 143.46. FTIR (KBr) 3400 cm^{-1}. HRMS (ESIMS): m/z calcd for $C_{13}H_{17}O_4$ $(M + H)^+$ 237.1121, $C_{13}H_{16}O_4Na$ $(M + Na)^+$ 259.0941, found 237.1157, 259.0923.

(1′*S*,3′*R*,4′*R*,5′*R*,7′*S* and 7′*R*)-*N*^{2}-Isobutyryl-9-and-7-{4′-hydroxy-3′-hydroxymethyl-1′-phenyl-2′,6′-dioxabicyclo[3.3.0]oct-7′-yl}-guanine 16a,b(2) and 17a,b(2). WNA-9αG (**16a(2)**): a white powder (78%). Mp 156−159 °C. ^{1}H NMR (270 MHz, CD_3OD) δ 1.23 (d, 6H, J = 6.9 Hz), 2.72 (pseudoquintet, 1H, J = 6.9 Hz), 3.09−3.29 (m, 2H), 3.65 (dd, 1H, J = 6.6, 12.2 Hz), 3.80−3.89 (m, 2H), 4.02 (dd, 1H, J = 2.6, 6.5 Hz), 4.63 (d, 1H, J = 4.3 Hz), 6.60 (dd, 1H, J = 4.3, 7.8 Hz), 7.28−7.42 (m, 3H), 7.64−7.67 (m, 2H), 8.40 (s, 1H). ^{13}C NMR (125 MHz, CD_3OD) δ 19.32, 36.98, 51.19, 63.70, 73.33, 83.82, 86.46, 91.56, 93.34, 121.35, 126.41, 128.74, 129.52, 140.01, 142.37, 145.33, 150.88, 157.55, 181.72. FTIR ($CHCl_3$) 3400, 1690 cm^{-1}. FABMS (m/z) 456 $(M + H)^+$. WNA-9βG (**16b(2)**): a white powder (91%). Mp 160−163 °C. ^{1}H NMR (270 MHz, CD_3OD) δ 1.22 (d, 3H, J = 4.6 Hz), 1.24 (d, 3H, J = 4.6 Hz), 2.73 (pseudoquintet, 1H, J = 6.9 Hz), 2.91 (dd, 1H, J = 5.6, 13.5 Hz), 3.06 (dd, 1H, J = 8.6, 13.5 Hz), 3.71 (dd, 1H, J = 5.6, 11.9 Hz), 3.91 (dd, 1H, J = 6.6, 12.2 Hz), 3.92 (dd, 1H, J = 4.0, 9.2 Hz), 4.06 (ddd, 1H, J = 2.3, 5.9, 8.6 Hz), 4.96 (d, 1H, J = 3.6 Hz), 6.48 (dd, 1H, J = 5.6, 8.6 Hz), 7.25−7.40 (m, 3H), 7.71−7.74 (m, 2H), 8.30 (s, 1H). ^{13}C NMR (125 MHz, CD_3OD) δ 19.33, 36.95, 50.18, 64.34, 73.72, 84.98, 87.69, 90.48, 93.22, 121.75, 126.64, 128.73, 129.44, 139.63, 141.50, 149.73, 150.26, 157.49, 181.73. FTIR ($CHCl_3$) 3400, 1690 cm^{-1}. FABMS (m/z) 456 $(M + H)^+$. WNA-7αG (**17a(2)**): a white powder (94%). Mp 157−160 °C. ^{1}H NMR (270 MHz, CD_3OD) δ 1.20 (d, 3H, J = 6.9 Hz), 1.22 (d, 3H, J = 6.9 Hz), 2.72 (pseudoquintet, 1H, J = 6.9 Hz), 3.09−3.22 (m, 2H), 3.62 (dd, 1H, J = 5.6, 11.8 Hz), 3.78−3.87 (m, 2H), 3.90 (d, 1H, J = 3.3 Hz), 4.70 (d, 1H, J = 3.3 Hz), 6.92 (dd, 1H, J = 3.3, 6.9 Hz), 7.25−7.41 (m, 3H), 7.63−7.66 (m, 2H), 8.68 (s, 1H). ^{13}C NMR (125 MHz, CD_3OD) δ 19.35, 29.54, 50.23, 63.68, 73.38, 84.06, 89.07, 91.88, 93.42, 121.61, 126.64, 128.73, 129.51, 142.29, 143.53, 149.21, 154.89, 159.26, 181.83. FTIR ($CHCl_3$) 3400, 1690 cm^{-1}. FABMS (m/z) 456 $(M + H)^+$. WNA-7βG (**17b(2)**): a white powder (88%). Mp 164−169 °C. ^{1}H NMR (270 MHz, CD_3OD) δ 1.17−1.19 (m, 6H), 2.86 (t, 1H, J = 6.3 Hz), 2.81 (dd, 3H, J = 5.6, 13.1 Hz), 3.15−3.27 (m, 2H), 2.94 (dd, 1H, J = 5.8, 13.7 Hz), 3.67 (t, 1H, J = 5.9 Hz), 3.83 (dd, 1H, J = 3.6, 9.2 Hz), 4.05 (ddd, 1H, J = 2.6, 5.9, 8.9 Hz), 5.02 (d, 1H, J = 4.0 Hz), 6.45 (dd, 1H, J = 5.9, 8.8 Hz), 7.63−7.73 (m, 3H), 7.79−7.82 (m, 2H), 8.34 (bs, 1H). ^{13}C NMR (125 MHz, CD_3OD) δ 19.35, 36.93, 51.19, 63.78, 73.80, 84.77, 90.72, 90.75, 93.41, 112.00, 126.77, 128.57, 129.31, 141.54, 145.33, 149.57, 154.56, 160.65, 181.86. FTIR ($CHCl_3$) 3400, 1690 cm^{-1}. FABMS (m/z) 456 $(M + H)^+$.

(1′*S*,3′*R*,4′*R*,5′*R*,7′*S* and 7′*R*)-*N*^{6}-Benzoyl-9-{4′-hydroxy-3′-hydroxymethyl-1′-phenyl-2′,6′-dioxabicyclo[3.3.0]oct-7′-yl}adenine 18a,b-(2). WNA-αA (**18a(2)**): a white powder (79%). Mp 125−128 °C. ^{1}H NMR (400 MHz, CD_3OD) δ 3.21 (dd, 1H, J = 6.37, 13.66 Hz), 3.29 (dd, 1H, J = 8.42, 13.85 Hz), 3.67 (dd, 1H, J = 5.99, 11.98 Hz), 3.83−3.89 (m, 2H), 3.95−4.53 (m, 1H), 4.73 (d, 1H, J = 3.74 Hz), 6.89 (dd, 1H, J = 6.18, 8.42 Hz), 7.31 (t, 1H, J = 7.30 Hz), 7.41 (t, 2H, J = 7.68 Hz), 7.57 (t, 2H, J = 7.30 Hz), 7.65 (t, 2H, J = 7.48 Hz), 7.70 (d, 2H, J = 7.30 Hz), 8.09 (d, 2H, J = 7.67 Hz), 8.75 (s, 1H), 8.86 (s, 1H). ^{13}C NMR (125 MHz, CD_3OD) δ 48.96, 63.71, 73.36, 83.95, 86.25, 91.41, 93.42, 109.52, 126.42, 128.74, 129.41, 129.53, 129.55, 134.18, 136.54, 141.10, 142.39, 151.32, 153.99, 164.61. FTIR (KBr) 3400, 1701, 1614, 1582 cm^{-1}. HRMS (ESIMS) m/z calcd for $C_{25}H_{24}N_5O_5$ $(M + H)^+$ 474.1772, found 472.1798. WNA-βA (**18b(2)**): a white powder (59%). Mp 126−128 °C. ^{1}H NMR (400 MHz, CD_3OD) δ 3.00 (dd, 1H, J = 6.37, 13.66 Hz), 3.51 (dd, 1H, J = 8.42, 13.85 Hz), 3.73 (dd, 1H, J = 5.99, 11.98 Hz), 3.91−3.95 (m, 2H), 4.13−4.17 (m, 1H), 5.02 (d, 1H, J = 3.74 Hz), 6.67 (dd, 1H, J = 6.18, 8.42 Hz), 7.29 (t, 1H, J = 7.30 Hz), 7.40 (t, 2H, J = 7.30 Hz), 7.56 (t, 2H, J = 7.30 Hz), 7.65 (t, 1H, J = 7.30 Hz), 8.06 (d, 2H, J = 7.30 Hz), 8.09 (d, 2H, J = 7.30 Hz), 8.63 (s, 1H), 8.81 (s, 1H). ^{13}C NMR (125 MHz, CD_3OD) δ 49.21, 63.66, 73.75, 84.63, 88.82, 91.33, 93.56, 106.37, 126.65, 128.71, 129.43, 129.77, 133.90, 141.76, 144.99, 151.29, 153.24, 168.54. FTIR (KBr) 3400, 1697, 1614, 1582 cm^{-1}. HRMS (ESIMS) m/z calcd for $C_{25}H_{24}N_5O_5$ $(M + H)^+$ 474.1772, found 472.1814.

(1′*S*,3′*R*,4′*R*,5′*R*,7′*S* and 7′*R*)-(4′-Hydroxy-3′-hydroxymethyl-1′-phenyl-2′,6′-dioxabicyclo[3.3.0]oct-7′-yl)thymine 19a,b(2). WNA-αT (**19a(2)**): a colorless foam (47%). ^{1}H NMR (270 MHz, CD_3OD) δ 2.16 (s, 3H), 2.74 (dd, 1H, J = 3.63, 14.84 Hz), 2.92−3.04 (m, 1H), 3.67 (dd, 1H, J = 6.92, 12.21 Hz), 3.80−3.92 (m, 2H), 4.11−4.16 (m, 1H), 4.57−4.62 (m, 1H), 6.61 (dd, 1H, J = 3.96, 6.60 Hz), 7.26−7.59 (m, 6H), 7.71 (d, 2H, J = 7.25 Hz), 8.17−8.24 (m, 1H), 8.27−8.31 (m, 2H). ^{13}C NMR (100 MHz, CD_3OD) δ 12.58, 48.69, 63.90, 73.44, 84.05, 87.10, 90.37, 93.41, 112.21, 126.30, 128.67, 129.50, 138.37, 142.70, 152.69, 166.31. FTIR (film) 3400, 1690 cm^{-1}. FABMS (m/z): 361 $[M + H]^+$. WNA-βT (**19b(2)**): a colorless foam (71%). ^{1}H NMR (600 MHz, CD_3OD) δ 1.91 (s, 3H), 2.71 (dd, 1H, J = 8.42, 13.76 Hz), 2.75 (dd, 1H, J = 6.03, 13.76 Hz), 3.68 (dd, 1H, J = 6.04, 12.07 Hz), 3.86−3.89 (m, 2H), 4.00−4.03 (m, 1H), 4.84 (d, 1H, J = 3.65 Hz), 6.29 (dd, 1H, J = 6.03, 8.43 Hz), 7.26 (t, 1H, J = 7.44 Hz), 7.35 (t, 2H, J = 7.44 Hz), 7.69 (t, 3H, J = 7.45 Hz). ^{13}C NMR (100 MHz, CD_3OD) δ 12.33, 49.21, 63.53, 73.69, 84.52, 90.08, 90.55, 93.18, 111.83, 126.51, 128.62, 129.35, 138.83, 141.54, 152.23, 166.40. FTIR (film) 3400, 1690 cm^{-1}. HRMS (ESIMS) m/z calcd for $C_{18}H_{21}N_2O_6$ $(M + H)^+$ 361.1394, found 361.1412.

(1′*S*,3′*R*,4′*R*,5′*R*,7′*S* and 7′*R*)-*N*^{4}-Benzoyl-1-(4′-hydroxy-3′-hydroxymethyl-1′-phenyl-2′,6′-dioxabicyclo[3.3.0]oct-7′-yl)-5-methylcytosine 20a,b(2). WNA-α^{m}C (**20a(2)**): a colorless foam (44%). ^{1}H NMR (270 MHz, CD_3OD) δ 2.16 (dd, 1H, J = 3.63, 14.84 Hz), 2.92−

3.04 (m, 1H), 3.67 (dd, 1H, J = 6.92, 12.21 Hz), 3.80−3.92 (m, 2H), 4.11−4.16 (m, 1H), 4.57−4.62 (m, 1H), 6.61 (dd, 1H, J = 3.96, 6.60 Hz), 7.26−7.59 (m, 6H), 7.71 (d, 2H, J = 7.25 Hz), 8.17−8.24 (m, 1H), 8.27−8.31 (m, 2H). ^{13}C NMR (125 MHz, CD_3OD): δ 23.51, 48.83, 56.67, 63.96, 73.42, 79.04, 82.46, 89.91, 107.21, 126.33, 127.60, 129.54, 133.51, 137.00, 140.45, 142.66, 149.59, 163.91, 172.42. FTIR (KBr) 3400, 1701, 1560 cm^{-1}. HRMS (ESIMS) m/z calcd for $C_{25}H_{26}N_3O_6$ (M + H)$^+$ 464.1816, found 464.1827. WNA-β^mC (**20b-(2)**): a colorless foam (72%). ^{1}H NMR (270 MHz, CD_3OD) δ 2.16 (s, 3H), 2.77−2.80 (m, 2H), 3.67 (dd, 1H, J = 5.61, 11.88 Hz), 3.88 (dd, 1H, J = 3.63, 8.25 Hz), 4.02 (dd, 1H, J = 2.31, 8.25 Hz), 4.88−4.91 (m, 1H), 6.31 (dd, 1H, J = 6.60, 7.26 Hz), 7.24−7.52 (m, 7H), 7.71 (d, 2H, J = 7.26 Hz), 7.91−7.93 (m, 1H), 8.26−8.30 (m, 2H). ^{13}C NMR (125 MHz, CD_3OD) δ 25.14, 49.30, 56.00, 63.52, 73.74, 84.59, 90.87, 93.30, 106.37, 126.58, 128.67, 129.40, 133.68, 136.96, 141.33, 141.61, 156.55, 165.91, 169.48. FTIR (KBr) 3400, 1703, 1568 cm^{-1}. HRMS (ESIMS) m/z calcd for $C_{25}H_{26}N_3O_6$ (M + H)$^+$ 464.1816, found 464.1812.

(1′*S*,3′*R*,4′*R*,5′*R*,7′*S* and 7′*R*)-*N*^{4}-Benzoyl-1-(4′-hydroxy-3′-hydroxymethyl-1′-phenyl-2′,6′-dioxabicyclo[3.3.0]oct-7′-yl)cytosine 21a,b-(2). WNA-αC (**21a(2)**): a colorless foam (34%). ^{1}H NMR (270 MHz, CD_3OD) δ 2.72 (dd, 1H, J = 4.5, 15.0 Hz), 3.07 (dd, 1H, J = 7.6, 15.0 Hz), 3.64 (dd, 1H, J = 6.6, 11.9 Hz), 3.79 (dd, 1H, J = 2.6, 11.9 Hz), 3.93 (dd, 1H, J = 4.2, 8.9 Hz), 4.05−4.12 (m, 1H), 4.77 (dd, 1H, J = 1.3, 2.0 Hz), 6.49 (dd, 1H, J = 5.0, 7.6 Hz), 7.25−7.72 (m, 9H), 7.96−8.00 (m, 2H), 8.68 (d, 1H, J = 7.6 Hz). ^{13}C NMR (100 MHz, *d*-DMSO) δ 48.84, 61.59, 71.47, 82.60, 87.42, 89.63, 91.19, 96.25, 125.26, 127.21, 128.11, 128.39, 128.42, 132.68, 133.13, 141.84, 145.13, 152.95, 163.11, 167.27. FTIR (KBr) 3321, 1684, 1659, 1485 cm^{-1}. ESIMS (m/z) 450 [M + H]$^+$. WNA-βC (**21b(2)**): a colorless foam (76% for tow steps). ^{1}H NMR (270 MHz, CD_3OD) δ 2.70 (dd, 1H, J = 7.92, 14.02 Hz), 3.01 (dd, 1H, J = 5.94, 14.02 Hz), 3.73−3.94 (m, 2H), 4.04−4.09 (m, 1H,), 4.94 (d, 1H, J = 3.63 Hz), 6.34 (dd, 2H, J = 5.94, 7.92 Hz), 7.23−7.70 (m, 9H), 7.96−8.00 (m, 2H), 8.40 (d, 1H, J = 7.30 Hz). ^{13}C NMR (100 MHz, CD_3OD) δ 50.39, 63.43, 73.66, 84.38, 91.42, 92.26, 93.36, 98.71, 126.52, 128.66, 129.16, 129.40, 129.82, 134.10, 134.67, 141.63, 147.03, 157.68, 165.00, 169.14. FTIR (KBr) 3381, 1653, 1560, 1487 cm^{-1}. HRMS (ESIMS) m/z calcd for $C_{24}H_{24}N_3O_6$ (M + H)$^+$ 450.1660, found 450.1683.

(1′*R*,3′*R*,4′*R*,5′*S*,7′*S*)-{4′-Hydroxy-3′-hydroxymethyl-2′,6′-dioxabicyclo[3.3.0]oct-7′-yl}thymine 22b(2). 0.2 M NaOH (2.3 mL, 0.468 mmol) was added to a solution of **22b(1)** (48 mg, 0.13 mmol) in THF/methanol = 9:1 (0.98 mL) at 0 °C. After stirring for 1 h at 0 °C, the reaction mixture was quenched with acetic acid and diluted with MeOH, and then the solvent was evaporated. The residue was purified by flash chromatography (silica gel, $CHCl_3/CH_3OH$ = 5:1) to give the diol compound as a colorless oil (37 mg, 99%): ^{1}H NMR (400 MHz, CD_3OD) δ 1.83 (s, 3H), 2.36 (ddd, 1H, J = 1.68, 8.61, 14.22 Hz), 2.80 (ddd, 1H, J = 4.87, 7.11, 14.22 Hz), 3.57 (dd, 1H, J = 4.87, 11.98 Hz), 3.70 (ddd, 1H, J = 2.25, 4.87, 8.98 Hz), 3.80 (dd, 1H, J = 2.25, 11.98 Hz), 3.88 (d, 1H, J = 4.68, 8.98 Hz), 4.82 (d, 1H, J = 4.68 Hz), 4.97 (dt, 1H, J = 1.68, 6.93 Hz), 6.90 (dd, 1H, J = 4.87, 8.61 Hz), 7.17 (s, 1H). ^{13}C NMR (125 MHz, CD_3OD) δ 14.45, 40.03, 62.54, 73.89, 82.18, 84.23, 85.71, 87.04, 110.32, 137.77, 152.99, 168.65. FTIR (film) 3081 cm^{-1}. ESIMS (m/z) 307 (M + Na)$^+$.

General Procedure of the Synthesis of the β-Cyanoethylphosphoramidite Precursors of WNA. DMTrCl (1.5 equiv) was added to a solution of the dihydroxyl derivative of WNA in pyridine, and the mixture was stirred for 1 h. The mixture was diluted with EtOAc and successively washed with water and brine. The organic layer was dried over Na_2SO_4 and evaporated, and then the residue was purified by flash chromatography (silica gel, $CHCl_3$−CH_3OH containing 0.5% pyridine) to produce the corresponding DMTr-protected WNA. iPr$_2$NP(Cl)OC$_2$H$_4$CN (6 equiv) was added to a solution of the above DMTr derivative of WNA and iPr$_2$NEt (3 equiv) in dry CH_2Cl_2 at 0 °C. After stirring for 60 min at the same temperature, the reaction mixture was quenched with sat. $NaHCO_3$ solution and extracted with AcOEt. The organic layer was separated, dried over Na_2SO_4, and evaporated. The residue was purified by flash chromatography (silica gel, hexane/AcOEt) to give the purified material, which was crystallized in hexane at −78 °C. The hexane was removed by decantation, and the solid material was dried in a vacuum for several hours.

(1*S*,3*R*,4*R*,5*R*)-3-Dimethoxytrithyloxymethyl-4-*O*-(*N*,*N*-diisopropyl-β-cyanoethylphosphoramidyl)-1-phenyl-2,6-dioxabicyclo[3.3.0]-octane WNA-H, 15(3): a white powder (77%). ^{1}H NMR (270 MHz, $CDCl_3$/TMS) δ 1.07 (d, 6H, J = 6.6 Hz), 1.08 (d, 2H, J = 6.6 Hz), 2.32−2.54 (m, 2H), 2.62 (t, 2H, J = 6.27 Hz), 3.36−3.59 (m, 4H), 3.80 (s, 6H), 3.81−4.05 (m, 2H), 4.11−4.33 (m, 4H), 4.40 (d, 0.5H, J = 3.96 Hz), 4.50 (d, 0.5H, J = 4.29 Hz), 6.82−6.85 (m, 4H), 7.16−7.39 (m, 10H), 7.46−7.51 (m, 2H), 7.57−7.64 (m, 2H). FTIR ($CHCl_3$) 2341.4 cm^{-1}. HRMS (ESIMS): m/z, calcd for $C_{43}H_{52}N_2O_7P$ (M + H)$^+$ 739.3507, found 739.3554.

(1′*S*,3′*R*,4′*R*,5′*R*,7′*S* and 7′*R*)-*N*^{2}-Isobutyryl-9-and-7-{3′-dimethoxytrithyloxymethyl-4′-*O*-(*N*,*N*-diisopropyl-β-cyanoethylphosphoramidyl)-1′-phenyl-2′,6′-dioxabicyclo[3.3.0]oct-7′-yl}guanine 16a,b(3) and 17a,b(3). WNA-9βG (**16b(3)**): a white powder (91%). ^{1}H NMR (270 MHz, $CDCl_3$) δ 1.17 (d, 6H, J = 6.6 Hz), 1.20 (d, 6H, J = 6.9 Hz), 1.25 (d, 3H, J = 3.3 Hz), 1.28 (d, 3H, J = 3.3 Hz), 2.38−2.51 (m, 2H), 2.63 (pseudoquintet, 0.5H, J = 6.9 Hz), 2.67 (pseudoquintet, 0.5H, J = 6.6 Hz), 2.95−3.12 (m, 1H), 3.22−3.28 (m, 1H), 3.40−3.73 (m, 4H), 3.79 (s, 3H), 3.80 (s, 3H), 4.07−4.35 (m, 3H), 5.22 (d, 0.5H, J = 2.6 Hz), 5.31 (d, 0.5H, J = 3.3 Hz), 6.32 (dd, 0.5H, J = 6.9, 7.6 Hz), 6.40 (dd, 0.5H, J = 6.6, 7.6 Hz), 6.82 (dd, 4H, J = 4.6, 8.6 Hz), 7.20−7.49 (m, 11H), 7.69−7.80 (m, 3H), 8.13 (s, 1H), 8.90 (bs, 1H), 12.0 (bs, 1H). WNA-9αG (**16a(3)**): a white powder (74%). ^{1}H NMR (270 MHz, $CDCl_3$) δ 1.17 (d, 6H, J = 6.6 Hz), 1.20 (d, 6H, J = 6.9 Hz), 1.25 (d, 3H, J = 3.3 Hz), 1.28 (d, 3H, J = 3.3 Hz), 2.31 (dd, 2H, J = 2.9, 6.9 Hz), 2.48 (t, 1H, J = 6.6 Hz), 2.93−3.28 (m, 2H), 3.40−3.57 (m, 4H), 3.73 (s, 3H), 3.74 (s, 3H), 4.00−4.34 (m, 3H), 5.20 (d, 1H, J = 2.6 Hz), 6.32 (dd, 0.5H, J = 6.9, 7.6 Hz), 6.40 (dd, 0.5H, J = 6.6, 7.6 Hz), 6.75−6.80 (m, 4H), 7.16−7.49 (m, 12H), 7.72−7.78 (m, 2H), 8.08 (s, 1H), 9.80 (bs, 1H), 12.2 (bs, 1H). WNA-7βG (**17b(3)**): a white powder (92%). ^{1}H NMR (270 MHz, $CDCl_3$) δ 1.17 (d, 6H, J = 6.6 Hz), 1.20 (d, 6H, J = 6.9 Hz), 1.25 (d, 3H, J = 3.3 Hz), 1.28 (d, 3H, J = 3.3 Hz), 2.31 (dd, 2H, J = 2.9, 6.9 Hz), 2.48 (t, 1H, J = 6.6 Hz), 2.93−3.28 (m, 2H), 3.40−3.57 (m, 4H), 3.76 (s, 3H), 3.77 (s, 3H), 4.00−4.34 (m, 3H), 5.20 (d, 1H, J = 2.6 Hz), 6.36 (dd, 0.5H, J = 6.9, 7.6 Hz), 6.44 (dd, 0.5H, J = 6.6, 7.6 Hz), 6.77−6.86 (m, 4H), 7.16−7.49 (m, 12H), 7.72−7.78 (m, 2H), 7.91 (s, 0.5H), 8.00 (s, 0.5H), 10.5 (bs, 1H), 12.3 (bs, 1H). WNA-7αG (**17a(3)**): a colorless oil (82%). ^{1}H NMR (270 MHz, $CDCl_3$) δ 1.07 (d, 6H, J = 6.9 Hz), 1.12 (d, 6H, J = 5.6 Hz), 1.25 (d, 3H, J = 4.3 Hz), 1.28 (d, 3H, J = 4.3 Hz), 3.00−3.24 (m, 2H), 3.33−3.62 (m, 4H), 3.76 (s, 3H), 3.77 (s, 3H), 4.04−4.30 (m, 3H), 5.77 (d, 1H, J = 2.6 Hz), 6.76−6.81 (m, 4H), 6.88 (dd, 1H, J = 2.9, 6.8 Hz), 6.91 (dd, 1H, J = 3.6, 7.2 Hz), 7.15−7.40 (m, 12H), 7.51−7.58 (m, 2H), 8.14 (s, 1H), 9.98 (bs, 1H), 12.3 (bs, 1H).

(1′*S*,3′*R*,4′*R*,5′*R*,7′*S* and 7′*R*)-*N*^{6}-Benzoyl-9-{3′-dimethoxytrithyloxymethyl-4′-*O*-(*N*,*N*-diisopropyl-β-cyanoethylphosphoramidyl)-1′-phenyl-2′,6′-dioxabicyclo[3.3.0]oct-7′-yl}adenine 18a,b(3). WNA-αA (**18a(3)**): a white powder (79%). ^{1}H NMR (400 MHz, $CDCl_3$/TMS): δ 0.87 (d, 2H, J = 6.74 Hz), 1.06 (dd, 5H, J = 3.56, 6.74 Hz), 1.11 (d, 2H, J = 6.92 Hz), 1.26 (d, 3H, J = 5.81, 6.78 Hz), 3.26−3.33 (m, 1H), 3.40−3.60 (m, 5H), 3.69−3.73 (m, 1H), 3.77 (s, 3H), 3.79 (s, 3H), 4.09−4.27 (m, 4H), 4.48 (d, 0.5H, J = 3.93 Hz), 4.95 (d, 0.5H, J = 3.74 Hz), 6.15 (s, 1H), 6.79−6.85 (m, 4H), 7.12−7.37 (m, 9H), 7.39−7.42 (m, 2H), 7.51−7.54 (m, 2H), 7.59−7.63 (m, 3H), 7.75 (s, 1H), 8.03 (d, 2H, J = 7.49 Hz), 8.69 (d, 1H, J = 4.49 Hz), 8.83 (d, 1H, J = 5.43 Hz), 9.01 (bs, 1H). FTIR (KBr) 2252, 1701, 1609 cm^{-1}. WNA-βA (**18b(3)**): a white powder (79%). ^{1}H NMR (400 MHz, $CDCl_3$/TMS) δ 0.87 (d, 2H, J = 6.74 Hz), 0.94 (d, 2H, J = 6.74 Hz), 1.07 (dd, 5H, J = 6.74, 9.73 Hz), 1.21−1.35 (m, 3H), 3.12−3.20 (m,

1H), 3.25−3.55 (m, 5H), 3.62−3.74 (m, 1H), 3.79 (s, 3H), 3.80 (s, 3H), 4.09−4.15 (m, 2H), 4.32−4.46 (m, 2H), 5.16 (d, 0.5H, J = 2.81 Hz), 5.17 (d, 0.5H, J = 3.56 Hz), 6.55 (dd, 0.5H, J = 6.74, 7.49 Hz), 6.63 (dd, 0.5H, J = 6.74, 7.67 Hz), 6.82 (d, 2H, J = 8.79 Hz), 6.83 (d, 2H, J = 8.98 Hz), 7.20−7.39 (m, 10H), 7.46−7.55 (m, 4H), 7.61 (t, 1H, J = 7.49 Hz), 7.76 (d, 1H, J = 6.93 Hz), 7.82 (d, 1H, J = 6.93 Hz), 8.03 (d, 2H, J = 7.68 Hz), 8.15 (s, 0.5H), 8.23 (s, 0.5H), 8.87 (d, 1H, J = 4.31 Hz), 9.00 (bs, 1H). FTIR (KBr) 2252, 1701, 1609 cm^{-1}.

(1′*S*,3′*R*,4′*R*,5′*R*,7′*S* and 7′*R*)-{3′-Dimethoxytrithyloxymethyl-4′-*O*-(*N*,*N*-diisopropyl-*β*-cyanoethylphosphoramidyl)-1′-phenyl-2′,6′-dioxabicyclo[3.3.0]oct-7′-yl}thymine 19a,b(3). WNA-αT (**19a(3)**): a white powder (37%). ^{1}H NMR (270 MHz, $CDCl_3$/TMS) δ 0.88 (d, 2H, J = 6.6 Hz), 0.99−1.13 (m, 6H), 1.16−1.38 (m, 4H), 2.04 (s, 3H), 2.34 (dd, 1H, J = 6.2, 7.8 Hz), 2.55 (t, 1H, J = 6.3 Hz), 2.62−2.73 (m, 1H), 2.92 (ddd, 1H, J = 2.6, 8.1, 14.9 Hz), 3.24−3.30 (m, 2H), 3.35−3.75 (m, 4H), 3.78 (s, 3H), 3.79 (s, 3H), 4.12 (dd, 2H, J = 6.9, 15.1 Hz), 4.23−4.36 (m, 2H), 4.55 (dd, 0.5H, J = 3.3 Hz), 4.66 (d, 0.5H, J = 3.9 Hz), 6.57 (dd, 1H, J = 4.9, 7.5 Hz), 6.79−6.83 (m, 4H), 7.20−7.37 (m, 10H), 7.43−7.49 (m, 4H), 7.76 (s, 1H), 7.80 (s, 1H). FTIR (KBr) 1690 cm^{-1}. WNA-βT (**19b(3)**): a white powder (76%). ^{1}H NMR (270 MHz, $CDCl_3$/TMS) δ 0.99−1.13 (m, 6H), 1.16−1.38 (m, 4H), 2.04 (s, 3H), 2.35 (dd, 1H, J = 6.2, 11.1 Hz), 2.62 (dd, 2H, J = 5.9, 14.1 Hz), 2.97−3.02 (m, 1H), 3.17−3.24 (m, 1H), 3.35−3.75 (m, 4H), 3.78 (s, 3H), 3.79 (s, 3H), 4.12 (dd, 2H, J = 6.9, 14.1 Hz), 4.21−4.37 (m, 4H), 4.91 (d, 0.5H, J = 3.6 Hz), 5.03 (d, 0.5H, J = 3.6 Hz), 6.21 (dd, 0.5H, J = 6.6, 8.5 Hz), 6.40 (dd, 0.5H, J = 6.6, 8.5 Hz), 6.80 (dd, 4H, J = 1.9, 8.8 Hz), 7.20−7.35 (m, 10H), 7.42−7.48 (m, 2H), 7.60 (dd, 2H J = 1.9, 9.2 Hz), 7.65 (dd, 1H, J = 1.9, 6.1 Hz), 8.20 (bs, 1H). FTIR ($CHCl_3$) 1690 cm^{-1}.

(1′*S*,3′*R*,4′*R*,5′*R*,7′*S* and 7′*R*)-*N*^{4}-Benzoyl-1-{3′-dimethoxytrithyloxymethyl-4′-*O*-(*N*,*N*-diisopropyl-*β*-cyanoethylphosphoramidyl)-1′-phenyl-2′,6′-dioxabicyclo[3.3.0]oct-7′-yl}-5-methylcytosine 20a,b(3). WNA- α^{m}C (**20a(3)**): a white powder (99%). ^{1}H NMR (270 MHz, $CDCl_3$/TMS) δ 0.90 (d, 2H, J = 6.6 Hz), 1.05−1.42 (m, 6H), 1.48−1.56 (m, 4H), 2.17 (s, 3H), 2.63−2.96 (m, 2H), 3.33−3.74 (m, 6H), 3.79 (s, 3H), 3.80 (s, 3H), 4.09−4.22 (m, 1H), 4.21−4.56 (m, 3H), 5.00−5.10 (m, 1H), 6.55−6.74 (m, 1H), 6.83 (dd, 4H, J = 2.31, 7.58 Hz), 7.18−7.77 (m, 18H), 8.33 (d, 2H, J = 7.59 Hz). FT-IR ($CHCl_3$): 2341, 1707, 1572 cm^{-1}. WNA- β ^{m}C (**20b(3)**) a white powder (67%). ^{1}H NMR (270 MHz, $CDCl_3$/TMS) δ 0.90 (d, 2H, J = 6.6 Hz), 1.05−1.42 (m, 6H), 1.48−1.56 (m, 4H), 2.19 (s, 3H), 2.48−2.89 (m, 2H), 3.00−3.19 (m, 2H), 3.33−3.74 (m, 4H), 3.79 (s, 3H), 3.80 (s, 3H), 4.01−4.09 (m, 1H), 4.21−4.38 (m, 3H), 4.95−5.08 (m, 1H), 6.23−6.41 (m, 1H), 6.83 (dd, 4H, J = 2.31, 7.58 Hz), 7.16−7.75 (m, 18H), 8.33 (d, 2H, J = 7.92 Hz). FTIR ($CHCl_3$) 2341, 1709, 1572 cm^{-1}.

(1′*S*,3′*R*,4′*R*,5′*R*,7′*S* and 7′*R*)-*N*^{4}-Benzoyl-1-{3′-dimethoxytrithyloxymethyl-4′-*O*-(*N*,*N*-diisopropyl-*β*-cyanoethylphosphoramidyl)-1′-phenyl-2′,6′-dioxabicyclo[3.3.0]oct-7′-yl}cytosine 21a,b(3). WNA-αC (**21a(3)**): a white powder (94%). ^{1}H NMR (270 MHz, $CDCl_3$/TMS) δ 1.01 (d, 2H, J = 6.81 Hz), 1.14−1.65 (m, 12H), 2.04−2.17 (m, 1H), 2.33−2.35 (m, 1H), 2.57−2.70 (m, 1H), 3.27−3.57 (m, 4H), 3.78 (s, 3H), 3.79 (s, 3H), 4.23−3.92 (m, 4H), 6.24−6.31 (m, 1H), 6.80 (d, 2H, J = 6.87 Hz), 6.81 (d, 2H, J = 6.76 Hz), 7.20−7.61 (m, 20H), 7.91 (d, 1H, J = 6.4 Hz). WNA-βC (**21b(3)**): a white powder (83%). ^{1}H NMR (270 MHz, $CDCl_3$/TMS) δ 0.86−0.90 (m, 2H), 0.93−1.32 (m, 12H), 2.02−2.08 (m, 1H), 2.34 (dd, 1H, J = 6.10, 10.88 Hz), 2.45−2.63 (m, 1H), 3.18−3.76 (m, 4H), 3.79 (s, 6H), 4.08−4.16 (m, 1H), 4.29−4.39 (m, 1H), 4.95−5.06 (m, 1H), 6.31−6.43 (m, 1H), 6.82 (dd, 4H, J = 1.65, 8.91 Hz), 7.20−7.64 (m, 18H), 7.29 (d, 1H, J = 7.92 Hz), 7.99 (d, 1H, J = 7.26 Hz), 8.19 (d, 1H, J = 7.26 Hz). ESIMS (m/z) 952.4 (M + H)$^+$.

(1′*S*,3′*R*,4′*R*,5′*R*,7′*S*)-{3′-Dimethoxytrithyloxymethyl-4′-*O*-(*N*,*N*-diisopropyl-*β*-cyanoethylphosphoramidyl)-2′,6′-dioxabicyclo[3.3.0]-oct-7′-yl}thymine 22b(3). H-WNA-βT (**22b(3)**): a white powder (66%). ^{1}H NMR (400 MHz, $CDCl_3$/TMS) δ 0.91 (d, 2H, J = 6.74 Hz), 1.09 (d, 6H, J = 6.74 Hz), 1.14 (d, 4H, J = 6.74 Hz), 1.85 (s, 1.5H), 1.87 (s, 1.5H), 2.34−2.45 (m, 1H), 2.52 (dd, 1H, J = 8.61, 13.1 Hz), 2.64 (t, 1H, J = 7.11 Hz), 2.72−2.85 (m, 1H), 3.05 (dd, 1H, J = 5.61, 10.3 Hz), 3.28−3.63 (m, 4H), 3.78 (s, 3H), 3.79 (s, 3H), 3.83−3.89 (m, 1H), 3.93−3.98 (m, 1H), 4.05−4.08 (m, 1H), 4.16−4.22 (m, 1H), 4.94 (t, 0.5H, J = 4.12 Hz), 5.02 (t, 0.5H, J = 4.50 Hz), 5.08−5.10 (m, 0.5H), 5.16−5.17 (m, 0.5H), 6.81 (dd, 4H, J = 1.31, 7.30 Hz), 6.95 (dd, 1H, J = 4.87, 8.42 Hz), 7.19 (t, 1H, J = 6.92 Hz), 7.22−7.30 (m, 2H), 7.33−7.38 (m, 4H), 7.46 (t, 2H, J = 7.11 Hz). FTIR (film): 2253, 1717, 1651 cm^{-1}. HRMS (ESIMS): m/z calcd for $C_{42}H_{52}N_4O_9P$ (M + H)$^+$ 787.3466, found 787.3469.

Table 3. Selected Chemical Shifts of ^{1}H and ^{13}C NMR of Diol Derivatives of WNA (**16(2)** and **17(2)**)[a]

	7-βG	9-βG	7-αG	9-αG
H-8[b]	8.39	8.28	8.68	8.40
C-anomeric[c]	90.72	87.69	89.07	86.46
C-4[c]	160.65	150.26	159.26	145.33
C-5[c]	112.00	121.75	112.61	121.35
C-8[b]	145.33	139.63	143.53	140.01

[a] ppm from TMS in CD_3OD. [b] ^{1}H NMR measured at 500 MHz. [c] ^{13}C NMR measured at 125 MHz.

Table 4. MALDI-TOF MS (negative mode) of the TFO Containing WNA Analogue (M^{-1} *m/z*)

TFO	WNA	calcd	found
23	WNA-9αG	5883.06	5886.0
23	WNA-7αG	5883.06	5882.64,
23	WNA-9βG	5883.06	5883.3
23	WNA-7βG	5883.06	5880.68
23	WNA-αA	5867.05	5866.79
23	WNA-βA	5867.05	5866.06
23	WNA-αT	5858.29	5858.3,
23	WNA-βT	5858.29	5857.91
25	WNA-βT, WNA-βT	5951.56	5955.46
23	WNA-α^{m}C	5857.06	5855.3
23	WNA-β^mC	5857.06	5859.97
23	WNA-αC	5845.06	5843.11
23	WNA-βC	5845.06	5843.44
23	WNA-H	5734.10	5730.50
23	H-WNA-βT	5782.01	5780.66

Determination of the Regio- and Stereochemistry of 16(2) and 17(2). N^7 or N^9 alkylation was determined based on different chemical shifts of guanine, in which signals of H-8, anomeric carbon, C-4, and C-8 of N^7-isomer appear more downfield than that of the N^9-isomer both in ^{1}H and ^{13}C NMR spectra. On the other hand, a signal of C-5 of the N^7-isomer appeared more upfield than that of the N^9-isomer.[27,28] Table 3 summarizes selected chemical shifts of each isomer.

Synthesis of the TFO Containing the WNA Analogue. The triplex-forming oligodeoxynucleotides incorporating the WNA analogue were synthesized by using an automated DNA synthesizer (Applied Biosystems 394 DNA/RNA Synthesizer) according to the standard protocol except for the use of DCI as the activator. Cleavage and deprotection of the synthesized oligomer were done in 28% NH_4OH at 55 °C for 5 h. HPLC conditions: column, Nacalai Tesque COSMOSIL5C18-AR-II; buffer A, 0.1 M TEAA; buffer B, CH_3CN. B, 10% to 40%/20 min, 40% to 100%/30 min, linear gradient; flow rate, 4 mL/min. A peak appeared at around t_R = 20 min was collected and freeze-dried. The DMTr protecting group was cleaved in 10% aqueous acetic acid at room temperature for 30 min, the resulting DMTr-OH was removed by washing with ether, and the solvents were lyophilized. Structure and purity of the synthesized TFO were confirmed by MALDI-TOF MS measurements (Table 4).

Purification of the Target Duplex. A mixture containing equal amounts of the complementary oligodeoxynucleotides was heated at 95 °C for 10 min, 55 °C for 30 min, 40 °C for 30 min, and 25 °C for 30 min. The duplex was purified by HPLC (Column: ZORBAX Oligo Column (6.2 mm ID × 80 mm, 5μm); buffer A, 20% CH_3CN, 80%

0.02 M sodium phosphate (pH = 7.0); buffer B, A + 1.0 M NaCl. B: 40% to 80%/15 min, 80% to 100%/20 min, linear gradient; flow rate, 1.0 mL/min) and by ethanol precipitation for desalination.

Gel-Shift Assay. TFOs were 5′ end-labeled by using [γ-^{32}P]ATP (4000 Ci/mmol, ICN Biomedicals, Inc.) and T4 polynucleotide kinase (500 U, TAKARA Bio, Inc.) in T4 Kinase buffer according to the standard protocol. After incubating for 45 min at 37 °C, 250 mM EDTA and TEN 100 buffer were added to the mixture, and then the mixture was purified with DE52 and DOWEX50. The purity of labeled TFO was checked by 15% denatured polyacrylamide gel in the presence of 10 M urea. The mixture of the TFO (10 nM) containing the corresponding ^{32}P-labeled TFO (40000 cpm) and target duplex (0−100 nM) was incubated in a buffer containing 20 mM Tris-HCl (pH = 7.5), 20 mM (or 5 mM) $MgCl_2$, 2.5 mM spermidine, and 10% sucrose for 12−15 h at 22 °C. The mixture was analyzed by electrophoresis with 15% nondenatured polyacrylamide gel at 10 °C for 6−7 h at 110 V. Gels were visualized by BAS2500, and each band was quantified. The stability constants (K_s) for each TFO were then calculated using the following equation, K_s = [Triplex]/([duplex][TFO]), and averaged data from those obtained by multiple experiments are shown in Tables 1 and 2.

Acknowledgment. This work was supported by Grant-in-Aid for Scientific Research (B) from Japan Society for the Promotion of Science (JSPS), CREST from Japan Science and Technology Corporation, and Advanced and Innovational Research Program in Life Sciences from the Ministry of Education, Culture, Sports, Science and Technology, the Japanese Government and Kyushu University P&P “Green Chemistry” Program.

Supporting Information Available: COSY and NOESY spectra for determination of stereochemistry of glycosidic bond of all WNA derivatives. This material is available free of charge via the Internet at http://pubs.acs.org.

JA037211Z